Noname manuscript No.
(will be inserted by the editor)

A wavelet collocation method for neutral delay differential equations on metric star graph

Mo Faheem · **Arshad Khan*** · **Fathalla A. Rihan**

the date of receipt and acceptance should be inserted later

Abstract This paper proposes a Haar wavelet collocation approach to solve neutral delay differential equations on a metric star graph (NDDE-MSG) with κ edges. The application of Haar wavelet, together with its integration on NDDE-MSG, yields a system of equations, which on solving gives unknown wavelet coefficients and subsequently the solution. The upper bound of the global error norm is established to demonstrate that the proposed method converges exponentially. We conduct some numerical experiments to test the computational convergence of our approach. In this study, the authors explore the numerical solution for NDDE on metric star graphs for the first time.

Keywords Haar wavelet · Neutral delay differential equations · Collocation method · Metric star graph · Convergence

Mathematics Subject Classification (2020) 65T60 · 65N35 · 65N15

1 Introduction

A particular class of delay differential equations (DDEs), neutral delay differential equations (NDDEs), are frequently used to model biological, physiological, chemical, and electronic processes, as well as transportation systems (controlling ships and aircraft), neural networks, and economic growth. There is great interest in neutral delay differential equation systems among researchers; refer [26] and references therein. In particular, epidemiology [8] experienced a delay due to the time interval between infection and the formation of new viruses; immunology [4] experienced a delay because of the duration of infectious and immunological periods; population dynamics [9] experienced the delay due to the life cycle phases. In [17], the authors used modified Euler sequences to prove the existence and uniqueness of the solution of NDDEs triggered by state-dependent delays. In [15], the authors used the concept of fixed point theory in F-metric space to demonstrate the existence and uniqueness of NDDEs with unbounded delay. The

Mo Faheem
School of Advanced Sciences, VIT-AP University, Andhra Pradesh-522237, India.
E-mail: mofaheem1110@gmail.com

Arshad Khan*
Department of Mathematics, Jamia Millia Islamia, New Delhi-110025, India.
E-mail: akhan2@jmi.ac.in

Fathalla A. Rihan
Department of Mathematical Sciences, College of Science, United Arab Emirates University, Al-Ain 17551, UAE.
E-mail: fathalla_rihan@hotmail.com

literature discusses the asymptotic behavior, existence, and uniqueness of higher-order differential equation solutions; see [10,1]. A rich literature exists for the numerical solution of NDDEs since analytical solutions are difficult to obtain due to delays. Some authors used Taylor series expansion to remove the delayed component from NDDEs and reduced them to ordinary differential equations; see [16,25]. While this technique maintains the stability criteria of DDEs, it also adds the error term associated with the Taylor series truncation to the overall error, resulting in an overall reduction in consistency. As a result, researchers developed numerical methods for addressing the delay term directly. The works of authors in [7,6] and references therein are particularly noteworthy.

The abovementioned applications motivated us to study neutral delay differential equations on the metric star graph. Indeed, investigating differential equations on the metric star graph is crucial to studying various natural phenomena. Partial differential equations (PDEs) on a graph can explain several other essential processes, such as the flow on gas pipeline networks [31] and the propagation of water waves in open channels [33]. The investigation of wind-induced vibrations in spider webs, the blackout of electricity distributions via connected wires, and the propagation of electrons can be easily studied by PDE-MSG, which can only travel along the atomic bonds of a connected structure because of excessive potential restrictions. A network-like system was used for the first time in the 1940s to study differential operators. Differential equations on network-like domains have their roots in the studies of Kron [18], as well as Ruedenberg and Scherr [27]. Numerous studies have been published on solving ODEs and PDEs on graphs; see [19,20].

On the other hand, wavelets have proven to be an effective tool for computation. The critical properties of wavelets, including compact support and well localization, make them straightforward. The use of wavelets is often associated with high-speed computations. As a key tool for investigating differential equations, wavelets are extensively used [2,32,23,28,24,13,29,3,11,14]. For example, Chebyshev cardinal wavelets have been utilized by Heydari and Razzaghi to solve time-fractional coupled Klein–Gordon–Schrödinger equations and fractional integro-differential equations involving the $\psi-$Caputo fractional derivative [12,13]. In the literature, several studies have addressed the solution of differential equations on graph using wavelets. For instance, a Haar wavelet method was developed by Faheem and Khan [5] in conjunction with the convergence analysis for fractional diffusion equations on graphs. We also refer to [21,30] and references therein for more information about wavelet collocation methods for differential equations on metric graphs. This paper approximates the solution to neutral delay differential equations on a metric star graph (NDDE-MSG) using Haar wavelet.

Consider the graph $\mathcal{G}(\mathcal{V},\mathcal{E})$ with a finite number of vertices (nodes) $\mathcal{V}=\{v_r\}_{r=0}^{\kappa}$ and edges $\mathcal{E}$. This study examines a metric star graph [22] with continuous edges $\mathcal{E}$. Thus, every edge $\mathcal{E}=\{e_r\}_{r=1}^{\kappa}$ has an open interval $(0,l_r)$ with $l_r>0$. An example of a metric star graph is shown in Figure 1. This paper analyzes the following NDDE-MSG:

$$\partial_t u_r(x,t)=F_r\big(x,t,u_r,u_r\big(x,t-\tau_r\big),\partial_x u_r(x,t),\partial_x u_r(x,t-\tau_{1,r}),\partial_{xx}u_r,\partial_{xx}u_r(x,t-\tau_{2,r})\big),\ \ x\in(0,l_r),t\in\big(t_0,t_f\big), \tag{1}$$

$$u_r(x,t)=\varphi_r(x,t),\quad t\le t_0, \tag{2}$$

$$u_r(0,t)=u_s(0,t),\quad r\neq s,r=1(1)\kappa,s=1,2,\ldots,\kappa, \tag{3}$$

$$\sum_{r=1}^{\kappa}\partial_x u_r(0,t)=0, \tag{4}$$

$$u_r\left(l_r,t\right)=0,1\le r\le\kappa, \tag{5}$$

where $F_r\in C\left([0,l_r]\times\left[t_0,t_f\right]\times\mathbb{R}^6;\mathbb{R}\right)$ is a Lipschitz function in last six arguments, $\varphi(x,t)\big(=\{\varphi_r(x,t)\}_{r=1}^{\kappa}\big)\in C\left(\overline{\mathcal{G}(\mathcal{V},\mathcal{E})}\times\left[t_0-\tau_r\left(x,t,u_r(x,t)\right),t_f\right];\mathbb{R}\right)$, and $\tau_r,\tau_{1,r},\tau_{2,r}$ are continuous functions on $[t_0,t_f]\times[0,l_r]\times\mathbb{R}$ such that $t-\tau_r\le t_f$, $t-\tau_{i,r}<t_f$, $i=1,2$. Equation (3) is known as the continuity condition, while

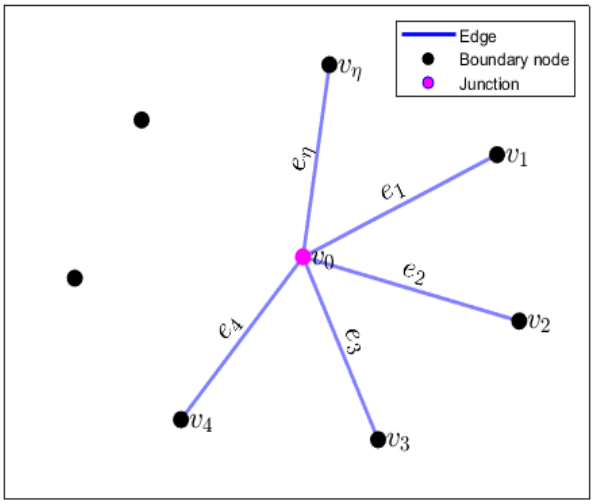

Fig. 1: Simplified schematic representation of a metric star graph consisting κ edges

equation (4) is known as the Kirchhoff condition. Our work focuses on solving equations (1) to (5) numerically using Haar wavelet. To the best of the authors' knowledge, this is the first attempt to solve NDDEs numerically on a metric star graph. Due to its accuracy and ease of implementation, we chose the Haar wavelet method over other numerical methods, such as finite difference schemes, collocation methods based on spline polynomials, and Galerkin methods. Generally, the aforementioned numerical methods have a constant order of convergence and require a large number of iterations or grid points to achieve desirable accuracy. In contrast, the Haar wavelet method exhibits exponential convergence and requires only a few grid points to produce accurate results. Since Haar wavelets uses piecewise functions as bases and have compact support, wavelets yield sparse matrices in the approximation, and hence significantly reducing the computational cost of the algorithm. Moreover, we use an integral operator approach, wherein the highest order mixed derivative is approximated in terms of Haar wavelets, and its integration is used to approximate the lower derivatives and the unknown variables. This approach effectively handles the continuity and Kirchhoff conditions of NDDEs on metric star graphs. This paper makes the following contributions:

- A metric star graph is used to study neutral delay differential equations for the first time.
- A Haar wavelet method has been developed to approximate the solution of NDDE-MSG. Both spatial and temporal derivatives are approximated using Haar wavelets and their integrations.
- Wavelet bases and their integration have been directly used to approximate the delayed terms presented in NDDE-MSG.
- The proposed method converges exponentially based on the error bound established for its theoretical applicability.

The paper is organized as follows. Section 2 provides a few basic definitions and preliminaries related to wavelets and metric star graphs. The Haar wavelet and function approximation are briefly discussed in Section 3. A general order integration of the Haar wavelet is given in Section 4. Section 5 discusses in detail about the numerical method for solving NDDE-MSG. In Section 6, we establish the convergence

analysis and error bounds for the approach. Section 7 presents five numerical examples based on NDDE-MSG using the method developed. The conclusion is provided in Section 8.

2 Preliminaries

The rest of the manuscript relies on some basic definitions and symbols which are provided in this section.

We define the following space on metric star graph $\mathcal{G}(\mathcal{V},\mathcal{E})$:

$$L^2(\mathcal{G}(\mathcal{V},\mathcal{E})) = \Pi_{r=1}^{\kappa} L^2(0,l_r), \tag{6}$$

with the following inner product

$$\langle u_r, v_r\rangle_{L^2(\mathcal{G}(\mathcal{V},\mathcal{E}))} = \sum_{r=1}^{\kappa} \langle u_r, v_r\rangle_{L^2(0,l_r)}, \tag{7}$$

where $L^2(0,l_r)$ be the Hilbert space. Let $C(\overline{\mathcal{G}})$ denotes the space of all continuous functions on $\overline{\mathcal{G}(\mathcal{V},\mathcal{E})}$ endowed with the norm

$$\|u\|_{C(\overline{\mathcal{G}})} = \sup_{1\le r\le \kappa} \|u\|_{\infty}, \tag{8}$$

where $\|.\|_{\infty}$ is the standard Chebyshev norm.

Definition 1 Multiresolution analysis (MRA) is defined as the sequence of subspaces $\{V^j\}$ of functions $f \in L^2(\mathbb{R})$ which meets the following axioms:

(i) $V^j \subset V^{j+1}$, $\forall j \in \mathbb{Z}$,
(ii) $\overline{\bigcup_{j\in\mathbb{Z}} V^j} = L^2(\mathbb{R})$,
(iii) The set $\{\phi(\cdot - k),\ k \in \mathbb{Z}\}$ forms an orthonormal basis for V^0,
(iv) If $f(\cdot) \in V^0 \Rightarrow f(2^j\cdot) \in V^j$.

Let $W^j = \{\psi_j^k,\ k, j \in \mathbb{Z}\}$ be defined as the subspace satisfying

$$V^j \perp W^j \ \text{ and } \ V^{j+1} = V^j \oplus W^j. \tag{9}$$

Applying equation (9) recursively yields

$$V^J = V^{J_0} \oplus \bigoplus_{j=J_0}^{J-1} W^j, \ \ J > J_0. \tag{10}$$

Now if we denote $P_{V^J} f$ as the projection of $f \in L^2(\mathbb{R})$ onto V^J then considering equation (10) yields

$$\begin{aligned} P_{V^J} f(x) &= \sum_k h_j^k \varphi_j^k(x), \\ P_{V^J} f(x) &= \sum_k h_{J_0}^k \varphi_{J_0}^k(x) + \sum_{k\in\mathbb{Z}} \sum_{j=1}^{J_0-1} g_j^k \psi_j^k(x), \end{aligned} \tag{11}$$

where $h_{J_0}^k$'s and g_j^k's can be determined by utilizing the scaling and wavelet functions as follows:

$$h_{J_0}^k = \int_{-\infty}^{\infty} f(x)\varphi_{J_0}^k(x)dx,\ g_j^k = \int_{-\infty}^{\infty} f(x)\psi_j^k(x)dx. \tag{12}$$

Definition 2 Multiresolution analysis (MRA) in two dimensions, is defined as the sequence of subspaces $\{V_2^{j_x,j_t}\}$ of functions $f \in L^2(\mathbb{R}\times\mathbb{R})$ which meets the following axioms:

(i) $V_2^{j_x,j_t} \subset V_2^{j_x+1,j_t+1}$, $\forall j_x, j_t \in \mathbb{Z}$,

(ii) $\overline{\bigcup_{j_x,j_t\in\mathbb{Z}} V_2^{j_x,j_t}} = L^2(\mathbb{R}\times\mathbb{R})$,

(iii) The set $\{\phi(\cdot - k_x, \cdot - k_t),\ k_x, k_t \in \mathbb{Z}\}$ forms an orthonormal basis for $V_2^{0,0}$,

(iv) If $f(\cdot,\cdot) \in V^0 \Rightarrow f(2^{j_x}\cdot, 2^{j_t}\cdot) \in V_2^{j_x,j_t}$, where $V_2^{j_x,j_t} = V^{j_x} \otimes V^{j_t}$ and $\otimes$ denotes the kronecker product.

Let $W_2^{j_x,j_t} = \{\psi_{j_x,j_t}^{k_x,k_t},\ j_x, j_t, k_x, k_t \in \mathbb{Z}\}$ be defined as the subspace satisfying

$$V_2^{j_x,j_t} \perp W_2^{j_x,j_t} \text{ and } V_2^{j_x+1,j_t+1} = V_2^{j_x,j_t} \oplus W_2^{j_x,j_t}. \tag{13}$$

Applying equation (13) recursively yields

$$V_2^{J_x,J_t} = V_2^{J_{x,0},J_{t,0}} \oplus \bigoplus_{\substack{j_x=J_x-1\\ j_t=J_t-1}}^{\substack{j_x=J_{x,0}\\ j_t=J_{t,0}}} W_2^{j_x,j_t},\ J_x > J_{x,0},\ J_t > J_{t,0}. \tag{14}$$

Now if denote $P_{V_2^{J_x,J_t}} f$ as the projection of $f \in L^2(\mathbb{R}\times\mathbb{R})$ onto $V_2^{J_x,J_t}$ then considering equation (14) gives

$$\begin{aligned} P_{V_2^{J_x,J_t}} f(x,t) &\approx \sum_{k_x,k_t} h_{j_x,j_t}^{k_x,k_t} \varphi_{j_x,j_t}^{k_x,k_t}(x,t), \\ P_{V_2^{J_x,J_t}} f(x,t) &\approx \sum_{k_x,k_t} h_{J_{x,0},J_{t,0}}^{k_x,k_t} \varphi_{J_{x,0},J_{t,0}}^{k_x,k_t}(x,t) + \sum_{k_x,k_t} \sum_{\substack{j_x=J_{x,0}\\ j_t=J_{t,0}}}^{\substack{J_x-1\\ J_t-1}} g_{j_x,j_t}^{k_x,k_t} \psi_{j_x,j_t}^{k_x,k_t}(x,t), \end{aligned} \tag{15}$$

where $h_{J_{x,0},J_{t,0}}^{k_x,k_t}$'s and $g_{j_x,j_t}^{k_x,k_t}$'s can be determined by utilizing the orthogonality of scaling and wavelet functions as:

$$h_{J_{x,0},J_{t,0}}^{k_x,k_t} = \int_{-\infty}^{\infty}\int_{-\infty}^{\infty} f(x,t)\varphi_{J_{x,0},J_{t,0}}^{k_x,k_t}(x,t)dxdt, \tag{16}$$

$$g_{j_x,j_t}^{k_x,k_t} = \int_{-\infty}^{\infty}\int_{-\infty}^{\infty} f(x,t)\psi_{j_x,j_t}^{k_x,k_t}(x,t)dxdt. \tag{17}$$

3 Haar wavelet

A function $\psi(x)$ is said to be a mother wavelet, if the following condition is satisfied:

$$2\pi \int_{-\infty}^{\infty} \frac{|\tilde{\psi}(\xi)|^2}{|\xi|} d\xi < \infty, \tag{18}$$

where $\tilde{\psi}(\xi)$ stands for the Fourier transform of $\psi(x)$. In general, we may reduced the condition (18) to the following weaker requirement:

$$\int_{-\infty}^{\infty} \psi(x)dx = 0. \tag{19}$$

That is, a function $\psi(x)$ is termed as mother wavelet if the total integral of the function is zero.

Wavelet is a set of functions constructed by the dilation and translation of mother wavelet $\psi(x)$ and defined as:

$$\psi_{d,T}(x) = |d|^{\frac{1}{2}} \psi\left(xd^{-1} - Td^{-1}\right), \quad T, d(\neq 0) \in \mathbb{R}. \tag{20}$$

The simplest example of wavelet is Haar wavelet which is constructed with help of the scaling function $\varphi(x) = 1$, if $x \in [0,1)$ and zero otherwise. The scaling function $\varphi(x)$ satisfies the following dilation equation:

$$\varphi(x) = \sqrt{2}\sum_k h_k \varphi(2x-k), \tag{21}$$

where $h_0 = h_1 = \frac{1}{\sqrt{2}}$ and $h_k = 0,\ \forall\, k > 1$.

The Haar mother wavelet can be define with the assistance of the scaling function $\varphi(x)$ as follows:

$$\psi(x) = \sum_k \sqrt{2} g_k \varphi(2x-k), \text{ with } g_k = (-1)^k \overline{h_{1-k}}, \tag{22}$$

where h_k and g_k are respectively the low pass and high pass filter coefficients calculated for Haar wavelet as: $g_0 = \frac{1}{\sqrt{2}}, g_1 = -\frac{1}{\sqrt{2}}$ and $g_k = 0,\ \forall\, k \neq \{0,1\}$.

Hence the Haar mother wavelet defined on $[0,1)$ as:

$$\psi(x) = \begin{cases} 1, & x \in \left[0, \frac{1}{2}\right), \\ -1, & x \in \left[\frac{1}{2}, 1\right), \\ 0, & \text{otherwise.} \end{cases} \tag{23}$$

Finally, we can obtained the Haar wavelet simply by dilating and translating the Haar mother wavelet function $\psi(x)$ as follows:

$$\psi_{j_x}^{k_x}(x) = \begin{cases} 1, & x \in \left[\frac{k_x}{2^{j_x}}, \frac{k_x+0.5}{2^{j_x}}\right), \\ -1, & x \in \left[\frac{k_x+0.5}{2^{j_x}}, \frac{k_x+1}{2^{j_x}}\right), \\ 0, & \text{otherwise,} \end{cases} \tag{24}$$

where $k_x = 0,1,2,\ldots,2^{j_x-1},\ j_x = 0,1,\ldots,J_x-1$, where J_x denotes the level of resolution.

Equivalently, we can define Haar wavelet for $i_x > 1$ as:

$$\psi_{i_x}(x) = \begin{cases} 1, & x \in \left[\frac{k_x}{2^{j_x}}, \frac{k_x+0.5}{2^{j_x}}\right), \\ -1, & x \in \left[\frac{k_x+0.5}{2^{j_x}}, \frac{k_x+1}{2^{j_x}}\right), \\ 0, & \text{otherwise} \end{cases} \quad \text{where } i_x = 2^{j_x} + k_x + 1, \tag{25}$$

$$\text{and } \psi_1(x) = \begin{cases} 1, & x \in [0,1), \\ 0, & \text{otherwise.} \end{cases} \tag{26}$$

Similarly, we can define Haar wavelet in temporal dimension for $i_t > 1$ as:

$$\psi_{i_t}(t) = \begin{cases} 1, & t \in \left[\frac{k_t}{2^{j_t}}, \frac{k_t+0.5}{2^{j_t}}\right), \\ -1, & t \in \left[\frac{k_t+0.5}{2^{j_t}}, \frac{k_t+1}{2^{j_t}}\right), \\ 0, & \text{otherwise} \end{cases} \quad \text{where } i_t = 2^{j_t} + k_t + 1, \tag{27}$$

$$\text{and } \psi_1(t) = \begin{cases} 1, & t \in [0,1), \\ 0, & \text{otherwise.} \end{cases} \tag{28}$$

The analytic expression of a function $u \in L^2[0,1)$ in terms of Haar wavelet can be obtained with the help of equation (11) as:

$$u(x) = h_0^0 \varphi_0^0(x) + \sum_{k_x}\sum_{j_x} g_{j_x}^{k_x} \psi_{j_x}^{k_x}(x). \tag{29}$$

The finest projection of u can be obtained by the terminated sum as follows:

$$u(x) \simeq P_{VJ_x} u(x) = h_0^0 \varphi_0^0(x) + \sum_{k_x} \sum_{j_x=j_{x,0}}^{J_x-1} g_{j_x}^{k_x} \psi_{j_x}^{k_x}(x) = \sum_{i_x=1}^{N_x} g_{i_x} \psi_{i_x}(x), \tag{30}$$

where the coefficients g_{i_x} 's can be found by

$$g_{i_x} = \int_{-\infty}^{\infty} u(x) \psi_{i_x}(x) dx. \tag{31}$$

Similarly, the analytic expression of a function $u \in L^2([0,1) \times [0,1))$ in terms of Haar wavelet can be found with the help of equation (15) as:

$$u(x,t) = h_{0,0}^{0,0} \varphi_{0,0}^{0,0}(x,t) + \sum_{k_x,k_t} \sum_{j_x,j_t} g_{j_x,j_t}^{k_x,k_t} \psi_{j_x}^{k_x}(x) \psi_{j_t}^{k_t}(t). \tag{32}$$

The finest projection of $u(x,t)$ can be obtained by the terminated sum as follows:

$$\begin{aligned} u(x,t) \simeq P_{V_2^{J_x,J_t}} u(x,t) &= h_{0,0}^{0,0} \varphi_{0,0}^{0,0}(x,t) + \sum_{k_x,k_t} \sum_{\substack{j_x=j_{x,0} \\ j_t=j_{t,0}}}^{\substack{J_x-1 \\ J_t-1}} g_{j_x,j_t}^{k_x,k_t} \psi_{j_x}^{k_x}(x) \psi_{j_t}^{k_t}(t) \\ &= \sum_{i_x=1}^{N_x} \sum_{i_t=1}^{N_t} g_{i_x,i_t} \psi_{i_x}(x) \psi_{i_t}(t), \end{aligned} \tag{33}$$

where the coefficients g_{i_x,i_t} 's can be found by

$$g_{i_x,i_t} = \int_{-\infty}^{\infty} \int_{-\infty}^{\infty} u(x,t) \psi_{i_x}(x) \psi_{i_t}(t) dx dt. \tag{34}$$

4 Integration of Haar wavelet

Let $\mathcal{J}_x^{(m)} \psi_{i_x}(x)$ and $\mathcal{J}_t^{(m)} \psi_{i_t}(t)$ denote the m^{th} order integrations of Haar wavelet against x and t respectively. Then using expression (25), we have

$$\mathcal{J}_x^{(m)} \psi_{i_x}(x) = \begin{cases} \frac{1}{m!}(x - \frac{k_x}{2^{j_x}})^m, & x \in [\frac{k_x}{2^{j_x}}, \frac{k_x+0.5}{2^{j_x}}), \\ \frac{1}{m!}\left(x - \frac{k_x}{2^{j_x}}\right)^m - 2\frac{1}{m!}\left(x - \frac{k_x+0.5}{2^{j_x}}\right)^m, & x \in \left[\frac{k_x+0.5}{2^{j_x}}, \frac{k_x+1}{2^{j_x}}\right), \\ \frac{1}{m!}\left(x - \frac{k_x}{2^{j_x}}\right)^m - 2\frac{1}{m!}\left(x - \frac{k_x+0.5}{2^{j_x}}\right)^m + \frac{1}{m!}\left(x - \frac{k_x+1}{2^{j_x}}\right)^m, & x \geq \frac{k_x+1}{2^{j_x}}. \end{cases} \tag{35}$$

In the same fashion, the integration of Haar wavelet in other direction is given by

$$\mathcal{J}_t^{(m)} \psi_{i_t}(t) = \begin{cases} \frac{1}{m!}\left(t - \frac{k_t}{2^{j_t}}\right)^m, & t \in \left[\frac{k_t}{2^{j_t}}, \frac{k_t+0.5}{2^{j_t}}\right), \\ \frac{1}{m!}\left(t - \frac{k_t}{2^{j_t}}\right)^m - 2\frac{1}{m!}\left(t - \frac{k_t+0.5}{2^{j_t}}\right)^m, & t \in \left[\frac{k_t+0.5}{2^{j_t}}, \frac{k_t+1}{2^{j_t}}\right), \\ \frac{1}{m!}\left(t - \frac{k_t}{2^{j_t}}\right)^m - 2\frac{1}{m!}\left(t - \frac{k_t+0.5}{2^{j_t}}\right)^m + \frac{1}{m!}\left(t - \frac{k_t+1}{2^{j_t}}\right)^m, & t \geq \frac{k_t+1}{2^{j_t}}. \end{cases} \tag{36}$$

5 Numerical method

Herein, we approximate the highest order mixed derivative of $u_r(x,t)$ in terms of Haar wavelet. Next, we approximate the lower order derivatives and unknown functions $u_r(x,t)$ in terms of the Haar wavelet and its integrations. Plugging the values of $u_r(x,t)$ along the derivatives in equation (1), the system of algebraic equations is obtained, which on solving yields undetermined wavelet coefficients and subsequently approximate solutions. Here, we develop the method for $l_r = 1,\ r = 1,2,\dots\kappa$ as described below.

We can approximate the mixed derivative $\partial_t\partial_{xx}u_r(x,t)$ in terms of Haar wavelet as:

$$\partial_t\partial_{xx}u_r(x,t) = \sum_{i_x=1}^{N_x}\sum_{i_t=1}^{N_t} g^r_{i_x,i_t}\psi_{i_x}(x)\psi_{i_t}(t). \tag{37}$$

Integrating equation (37) against t, yields

$$\partial_{xx}u_r(x,t) = \sum_{i_x=1}^{N_x}\sum_{i_t=1}^{N_t} g^r_{i_x,i_t}\psi_{i_x}(x)\mathfrak{I}_t^{(1)}\psi_{i_t}(t) + \partial_{xx}u_r(x,0). \tag{38}$$

In a similar way, subsequent integrations of equation (38) with respect to x, provides

$$\partial_x u_r(x,t) = \sum_{i_x=1}^{N_x}\sum_{i_t=1}^{N_t} g^r_{i_x,i_t}\mathfrak{I}_x^{(1)}\psi_{i_x}(x)\mathfrak{I}_t^{(1)}\psi_{i_t}(t) + \partial_x u_r(x,0) - \partial_x u_r(0,0) + \partial_x u_r(0,t), \tag{39}$$

$$u_r(x,t) = \sum_{i_x=1}^{N_x}\sum_{i_t=1}^{N_t} g^r_{i_x,i_t}\mathfrak{I}_x^{(2)}\psi_{i_x}(x)\mathfrak{I}_t^{(1)}\psi_{i_t}(t) + u_r(x,0) - u_r(0,0) - x\partial_x u_r(0,0) + x\partial_x u_r(0,t) + u_r(0,t). \tag{40}$$

If we plug $x = 1$ into equation (40) and add up all the values, we obtain

$$\begin{aligned}\sum_{r=1}^{\kappa} u_r(1,t) &= \sum_{r=1}^{\kappa}\sum_{i_x=1}^{N_x}\sum_{i_t=1}^{N_t} g^r_{i_x,i_t}\mathfrak{I}_x^{(2)}\psi_{i_x}(1)\mathfrak{I}_t^{(1)}\psi_{i_t}(t) + \sum_{r=1}^{\kappa}(u_r(1,0) - u_r(0,0) - \partial_x u_r(0,0))\\ &\quad + \sum_{r=1}^{\kappa}\partial_x u_r(0,t) + \sum_{r=1}^{\kappa} u_r(0,t),\\ \Rightarrow u_r(0,t) &= -\frac{1}{\kappa}\sum_{r=1}^{\kappa}\sum_{i_x=1}^{N_x}\sum_{i_t=1}^{N_t} g^r_{i_x,i_t}\mathfrak{I}_x^{(2)}\psi_{i_x}(1)\mathfrak{I}_t^{(1)}\psi_{i_t}(t) - \frac{1}{\kappa}\sum_{r=1}^{\kappa}(u_r(1,0) - u_r(0,0) - \partial_x u_r(0,0)), 1 \le r \le \kappa.\end{aligned} \tag{41}$$

Again, for the equation (40), set x equal to 1, and then after simplifying, we obtain

$$\partial_x u_r(0,t) - \partial_x u_r(0,0) = -\sum_{i_x=1}^{N_x}\sum_{i_t=1}^{N_t} g^r_{i_x,i_t}\mathfrak{I}_x^{(2)}\psi_{i_x}(1)\mathfrak{I}_t^{(1)}\psi_{i_t}(t) - u_r(1,0) + u_r(0,0) + u_r(0,t). \tag{42}$$

Now, from equations (40), (41) and (42), we get

$$\begin{aligned}u_r(x,t) &= \sum_{i_x=1}^{N_x}\sum_{i_t=1}^{N_t} g^r_{i_x,i_t}\mathfrak{I}_x^{(2)}\psi_{i_x}(x)\mathfrak{I}_t^{(1)}\psi_{i_t}(t) - \sum_{i_x=1}^{N_x}\sum_{i_t=1}^{N_t} g^r_{i_x,i_t}x\mathfrak{I}_x^{(2)}\psi_{i_x}(1)\mathfrak{I}_t^{(1)}\psi_{i_t}(t)\\ &\quad - \frac{1}{\kappa}\sum_{r=1}^{\kappa}\sum_{i_x=1}^{N_x}\sum_{i_t=1}^{N_t} g^r_{i_x,i_t}(1-x)\mathfrak{I}_x^{(2)}\psi_{i_x}(1)\mathfrak{I}_t^{(1)}\psi_{i_t}(t) - \frac{1}{\kappa}\sum_{r=1}^{\kappa}(1-x)(u_r(1,0) - u_r(0,0) - \partial_x u_r(0,0))\\ &\quad + u_r(x,0) + (x-1)u_r(0,0) - xu_r(1,0).\end{aligned} \tag{43}$$

Again differentiation of equation (43) yields

$$\partial_t u_r(x,t) = \sum_{i_x=1}^{N_x}\sum_{i_t=1}^{N_t} g^r_{i_x,i_t} \mathcal{I}_x^{(2)}\psi_{i_x}(x)\psi_{i_t}(t) - \sum_{i_x=1}^{N_x}\sum_{i_t=1}^{N_t} g^r_{i_x,i_t} x\mathcal{I}_x^{(2)}\psi_{i_x}(1)\psi_{i_t}(t)$$
$$- \frac{1}{\kappa}\sum_{r=1}^{\kappa}\sum_{i_x=1}^{N_x}\sum_{i_t=1}^{N_t} g^r_{i_x,i_t}(1-x)\mathcal{I}_x^{(2)}\psi_{i_x}(1)\psi_{i_t}(t). \tag{44}$$

Also, using equation (41) in (39) gives

$$\partial_x u_r(x,t) = \sum_{i_x=1}^{N_x}\sum_{i_t=1}^{N_t} g^r_{i_x,i_t}\left(\mathcal{I}_x^{(1)}\psi_{i_x}(x) - \mathcal{I}_x^{(2)}\psi_{i_x}(1)\right)\mathcal{I}_t^{(1)}\psi_{i_t}(t) - \frac{1}{\kappa}\sum_{r=1}^{\kappa}\sum_{i_x=1}^{N_x}\sum_{i_t=1}^{N_t} g^r_{i_x,i_t}\mathcal{I}_x^{(2)}\psi_{i_x}(1)\mathcal{I}_t^{(1)}\psi_{i_t}(t)$$
$$+ \partial_x u_r(x,0) - u_r(1,0) + u_r(0,0) + \frac{1}{\kappa}\sum_{r=1}^{\kappa}(u_r(1,0) - u_r(0,0)). \tag{45}$$

Now, replace t by $t-\tau_{2,r},\ t-\tau_r$, and $t-\tau_{1,r}$ in equations (38), (43) and (45), respectively yields

$$\partial_{xx} u_r(x,t-\tau_{2,r}) = \sum_{i_x=1}^{N_x}\sum_{i_t=1}^{N_t} g^r_{i_x,i_t}\psi_{i_x}(x)\mathcal{I}_t^{(1)}\psi_{i_t}(t-\tau_{2,r}) + \partial_{xx}u_r(x,0), \tag{46}$$

$$u_r(x,t-\tau_r) = \sum_{i_x=1}^{N_x}\sum_{i_t=1}^{N_t} g^r_{i_x,i_t}\mathcal{I}_x^{(2)}\psi_{i_x}(x)\mathcal{I}_t^{(1)}\psi_{i_t}(t-\tau_r) - \sum_{i_x=1}^{N_x}\sum_{i_t=1}^{N_t} g^r_{i_x,i_t} x\mathcal{I}_x^{(2)}\psi_{i_x}(1)\mathcal{I}_t^{(1)}\psi_{i_t}(t-\tau_r)$$
$$- \frac{1}{\kappa}\sum_{r=1}^{\kappa}\sum_{i_x=1}^{N_x}\sum_{i_t=1}^{N_t} g^r_{i_x,i_t}(1-x)\mathcal{I}_x^{(2)}\psi_{i_x}(1)\mathcal{I}_t^{(1)}\psi_{i_t}(t-\tau_r) - \frac{1}{\kappa}\sum_{r=1}^{\kappa}(1-x)(u_r(1,0) - u_r(0,0)$$
$$- \partial_x u_r(0,0)) + u_r(x,0) + (x-1)u_r(0,0) - xu_r(1,0), \tag{47}$$

$$\partial_x u_r(x,t-\tau_{1,r}) = \sum_{i_x=1}^{N_x}\sum_{i_t=1}^{N_t} g^r_{i_x,i_t}(\mathcal{I}_x^{(1)}\psi_{i_x}(x) - \mathcal{I}_x^{(2)}\psi_{i_x}(1))\mathcal{I}_t^{(1)}\psi_{i_t}(t-\tau_{1,r}) - \frac{1}{\kappa}\sum_{r=1}^{\kappa}\sum_{i_x=1}^{N_x}\sum_{i_t=1}^{N_t} g^r_{i_x,i_t}\mathcal{I}_x^{(2)}\psi_{i_x}(1)$$
$$\times \mathcal{I}_t^{(1)}\psi_{i_t}(t-\tau_{1,r}) + \partial_x u_r(x,0) - u_r(1,0) + u_r(0,0) + \frac{1}{\kappa}\sum_{r=1}^{\kappa}(u_r(1,0) - u_r(0,0)). \tag{48}$$

Substituting equations (38), (43)-(48) in equation (1) and collocating at $x_{\theta_1} = \frac{\theta_1 - 0.5}{N_x}, t_{\theta_2} = \frac{\theta_2 - 0.5}{N_t}$, where $\theta_1 = 1,2,\ldots,N_x, \theta_2 = 1,2,\ldots,N_t$, forms the system of $\kappa\left((N_x)^2 \times (N_t)^2\right)$ nonlinear algebraic equations. Solving the resulting system provides undetermined wavelet coefficients $g^r_{i_x,i_t}$. These coefficient values when substituted in equation (43) yield the required approximation.

6 Convergence

In this section, we examine upper estimate of the error norm for the described method. We now write equation (43) in analytic form in order to demonstrate that the proposed method converges:

$$u_r(x,t) = \sum_{i_x=1}^{\infty}\sum_{i_t=1}^{\infty} g^r_{i_x,i_t}\mathcal{I}_x^{(2)}\psi_{i_x}(x)\mathcal{I}_t^{(1)}\psi_{i_t}(t) - \sum_{i_x=1}^{\infty}\sum_{i_t=1}^{\infty} g^r_{i_x,i_t}\mathcal{I}_x^{(2)}\psi_{i_x}(1)\mathcal{I}_t^{(1)}\psi_{i_t}(t)$$
$$- \frac{1}{\kappa}\sum_{r=1}^{\kappa}\sum_{i_x=1}^{\infty}\sum_{i_t=1}^{\infty} g^r_{i_x,i_t}(1-x)\mathcal{I}_x^{(2)}\psi_{i_x}(1)\mathcal{I}_t^{(1)}\psi_{i_t}(t) + \mathscr{B}(x,t), \tag{49}$$

where $\mathscr{B}(x,t)$ represents the function containing boundary terms.

Lemma 1 *Let $u_r(x,t) \in L^2((0,l_r)\times(0,1))$ with $l_r = 1$ such that $|\partial_{tt}\partial_{xxx}u_r(x,t)| \le \Re_r, \forall (x,t) \in (0,1)\times(0,1)$ and $\Re_r > 0$, $r = 1(1)\kappa$. If $\partial_t\partial_{xx}u_r(x,t) = \sum_{i_x=1}^{\infty}\sum_{i_t=1}^{\infty} g^r_{i_x,i_t}\psi_{i_x}(x)\psi_{i_t}(t)$, then the following inequality holds:*

$$\sum_{r=1}^{\kappa} \left|g^r_{i_x,i_t}\right| \le 2^{-2(j_x+j_t+1)}\kappa\Re, \tag{50}$$

where $\Re = \max_{1\le r\le\kappa} \Re_r$.

Proof We have

$$\partial_t\partial_{xx}u_r(x,t) = \sum_{i_x=1}^{\infty}\sum_{i_t=1}^{\infty} g^r_{i_x,i_t}\psi_{i_x}(x)\psi_{i_t}(t),$$
$$g^r_{i_x,i_t} = \int_0^1\int_0^1 \partial_t\partial_{xx}u_r(x,t)\psi_{i_x}(x)\psi_{i_t}(t)dxdt = \langle\psi_{i_x}(x), \langle\partial_t\partial_{xx}u_r(x,t), \psi_{i_t}(t)\rangle\rangle.$$

Now

$$\begin{aligned}\langle\partial_t\partial_{xx}u_r(x,t), \psi_{i_t}(t)\rangle &= \int_0^1 \partial_t\partial_{xx}u_r(x,t)\psi_{i_t}(t)dt\\ &= \int_{\frac{k_t}{2^{j_t}}}^{\frac{k_t+0.5}{2^{j_t}}} \partial_t\partial_{xx}u_r(x,t)dt - \int_{\frac{k_t+0.5}{2^{j_t}}}^{\frac{k_t+1}{2^{j_t}}} \partial_t\partial_{xx}u_r(x,t)dt\\ &= \frac{1}{2^{j_t+1}}\partial_t\partial_{xx}u_r(x,\chi_1) - \frac{1}{2^{j_t+1}}\partial_t\partial_{xx}u_r(x,\chi_2).\end{aligned}$$

Here the mean value theorem for integral is employed for $\chi_1 \in \left(k_t2^{-j_t}, (k_t+0.5)2^{-j_t}\right)$ and $\chi_2 \in ((k_t+0.5)2^{-j_t}, (k_t+1)2^{-j_t})$. Again applying mean value theorem for $\chi \in (\chi_1,\chi_2)$, we have

$$\langle\partial_t\partial_{xx}u_r(x,t), \psi_{i_t}(t)\rangle = \frac{1}{2^{j_t+1}}(\chi_1-\chi_2)\,\partial_{tt}\partial_{xx}u_r(x,\chi).$$

Now

$$\begin{aligned}\langle\psi_{i_x}(x), \langle\partial_t\partial_{xx}u_r(x,\chi), \psi_{i_t}(t)\rangle\rangle &= \frac{1}{2^{j_t+1}}(\chi_1-\chi_2)\int_0^1 \partial_{tt}\partial_{xx}u_r(x,\chi)\psi_{i_x}(x)dx\\ &= \frac{1}{2^{j_t+1}}(\chi_1-\chi_2)\left(\int_{\frac{k_x}{2^{j_x}}}^{\frac{k_x+0.5}{2^{j_x}}} \partial_{tt}\partial_{xx}u_r(x,\chi)dx - \int_{\frac{k_x+0.5}{2^{j_x}}}^{\frac{k_x+1}{2^{j_x}}} \partial_{tt}\partial_{xx}u_r(x,\chi)dx\right)\\ &= \frac{(\chi_1-\chi_2)}{2^{j_x+j_t+2}}\left(\partial_{tt}\partial_{xx}u_r(\omega_1,\chi) - \partial_{tt}\partial_{xx}u_r(\omega_2,\chi)\right).\end{aligned} \tag{51}$$

The abovementioned relation is attained by utilizing mean value theorem, provided $\omega_1 \in \left(k_x2^{-j_x}, (k_x+0.5)2^{-j_x}\right)$ and $\omega_2 \in \left((k_x+0.5)2^{-j_x}, (k_x+1)2^{-j_x}\right)$. Again applying mean value theorem for $\omega \in (\omega_1,\omega_2)$, we obtain

$$\langle\psi_{i_x}(x), \langle\partial_t\partial_{xx}u_r(x,t), \psi_{i_t}(t)\rangle\rangle = \frac{1}{2^{j_x+j_t+2}}(\chi_1-\chi_2)(\omega_1-\omega_2)\,\partial_{tt}\partial_{xxx}u_r(\omega,\chi).$$

Therefore, we have

$$\begin{aligned}\left|g^r_{i_x,i_t}\right| &= \frac{1}{2^{j_x+j_t+2}}|\chi_2-\chi_1||\omega_2-\omega_1||\partial_{tt}\partial_{xxx}u_r(\omega,\chi)|,\\ \left|g^r_{i_x,i_t}\right| &\le 2^{-2(j_x+j_t+1)}\Re_r,\\ \sum_{r=1}^{\kappa}\left|g^r_{i_x,i_t}\right| &\le 2^{-2(j_x+j_t+1)}\kappa\Re,\end{aligned}$$

where $\Re = \max_{1\le r\le\kappa} \Re_r$.

Lemma 2 *Let $u_r(x,t)$ be the accurate solution of NDDE-MSG (1) and $P_{V_2^{J_x,J_t}}u_r(x,t)$ be the projection of analytic solution such that $|\partial_{tt}\partial_{xxx}u_r(x,t)| \leq \Re_r$, $\forall\ (x,t) \in (0,1)\times(0,1)$ and $\Re_r > 0, r = 1(1)\kappa$ and $\partial_t\partial_{xx}u_r(x,t) = \sum_{i_x=1}^{\infty}\sum_{i_t=1}^{\infty} g^r_{i_x,i_t}\psi_{i_x}(x)\psi_{i_t}(t)$, then the following inequality holds:*

$$\sum_{r=1}^{\kappa} \|u_r(x,t) - P_{V_2^{J_x,J_t}}u_r(x,t)\|_{L^2(0,l_r)} \leq \Theta_1 2^{-4J_x-3J_t}, \tag{52}$$

where Θ_1 is a constant given in the proof below.

Proof Denote $\sum_{j_x=J_x+1}^{\infty}\sum_{i_x=2^{j_x}}^{j_x+1}\sum_{j_t=J_t+1}^{\infty}\sum_{i_t=2^{j_t}}^{2^{j_t+1}-1} := \underset{j_x,i_x,j_t,i_t}{\Omega}$. Then, we have

$$\begin{aligned}\sum_{r=1}^{\kappa}\left\|\left(u_r(x,t) - P_{V_2^{J_x,J_t}}u_r(x,t)\right)\right\|_{L^2(0,l_r)} &= \sum_{r=1}^{\kappa}\left\|\underset{j_x,i_x,j_t,i_t}{\Omega} g^r_{i_x,i_t}\left(\mathcal{J}_x^{(2)}\psi_{i_x}(x)\mathcal{J}_t^{(1)}\psi_{i_t}(t) - x\mathcal{J}_x^{(2)}\psi_{i_x}(1)\mathcal{J}_t^{(1)}\psi_{i_t}(t)\right)\right.\\ &\left. - \frac{1}{\kappa}\underset{j_x,i_x,j_t,i_t}{\Omega}\sum_{r=1}^{\kappa} g^r_{i_x,i_t}(1-x)\mathcal{J}_x^{(2)}\psi_{i_x}(1)\mathcal{J}_t^{(1)}\psi_{i_t}(t)\right\|_{L^2(0,l_r)}.\end{aligned} \tag{53}$$

Using Minkowski and Hölder inequalities, we have

$$\begin{aligned}\sum_{r=1}^{\kappa}\|u_r(x,t) - P_{V_2^{J_x,J_t}}u_r(x,t)\|_{L^2(0,l_r)} \leq \sum_{r=1}^{\kappa}\underset{j_x,i_x,j_t,i_t}{\Omega}|g^r_{i_x,i_t}|&\left(\left(\int_0^1|\mathcal{J}_x^{(2)}\psi_{i_x}(x)|^2dx\right)^{\frac{1}{2}}\left(\int_0^1|\mathcal{J}_t^{(1)}\psi_{i_t}(t)|^2dt\right)^{\frac{1}{2}}\right.\\ &+\left(\int_0^1|x\mathcal{J}_x^{(2)}\psi_{i_x}(1)|^2dx\right)^{\frac{1}{2}}\left(\int_0^1|\mathcal{J}_t^{(1)}\psi_{i_t}(t)|^2dt\right)^{\frac{1}{2}}\\ &\left.+\left(\int_0^1|(1-x)\mathcal{J}_x^{(2)}\psi_{i_x}(1)|^2dx\right)^{\frac{1}{2}}\left(\int_0^1|\mathcal{J}_t^{(1)}\psi_{i_t}(t)|^2dt\right)^{\frac{1}{2}}\right).\end{aligned} \tag{54}$$

Now consider

$$\begin{aligned}\mathcal{J}_x^{(m)}\psi_{i_x}(x) =& \frac{1}{\Gamma(m)}\int_0^x (x-s)^m\psi_{i_s}(s)ds\\ =& \frac{1}{\Gamma(m)}\left(\int_{\frac{k_x}{2^{j_x}}}^{\frac{k_x+0.5}{2^{j_x}}}(x-s)^m ds - \int_{\frac{k_x+0.5}{2^{j_x}}}^{\frac{k_x+1}{2^{j_x}}}(x-s)^m ds\right)\\ =& \frac{1}{(m+1)\Gamma(m)}\left(\left(x-\frac{k_x}{2^{j_x}}\right)^{m+1} - 2\left(x-\frac{k_x+0.5}{2^{j_x}}\right)^{m+1} + \left(x-\frac{k_x+1}{2^{j_x}}\right)^{m+1}\right),\\ |\mathcal{J}_x^{(m)}\psi_{i_x}(x)| \leq& \mathtt{A}2^{-j_x(m+1)},\end{aligned} \tag{55}$$

where $\mathtt{A} = \max\limits_{y\in(0,1)}\left|\frac{y^{m+1}-2(y-0.5)^{m+1}+(y-1)^{m+1}}{(m+1)\Gamma(m)}\right|$, $y = 2^{j_x}x - k_x$. Therefore, we have

$$|\mathcal{J}_x^{(1)}\psi_{i_x}(x)| \leq \mathtt{A}2^{-2j_x},\ \ |\mathcal{J}_x^{(2)}\psi_{i_x}(x)| \leq \mathtt{A}2^{-3j_x}, \text{ and } |\mathcal{J}_t^{(1)}\psi_{i_t}(t)| \leq \mathtt{A}2^{-2j_t}. \tag{56}$$

Now from equations (54) and (56), we obtain

$$\begin{aligned}\sum_{r=1}^{\kappa}\|u_r(x,t) - P_{V_2^{J_x,J_t}}u_r(x,t)\|_{L^2(0,l_r)} \leq& \underset{j_x,i_x,j_t,i_t}{\Omega}\frac{3\kappa\mathtt{A}^2\Re}{4}2^{-5j_x-4j_t}\\ =& \frac{3\kappa\Re\mathtt{A}^2}{4}\sum_{j_x=J_x+1}^{\infty}\sum_{i_x=2^{j_x}}^{2^{j_x+1}-1}2^{-5j_x}\sum_{j_t=J_t+1}^{\infty}2^{-3j_t}\end{aligned}$$

$$= \frac{3\kappa\Re\mathtt{A}^2 2^{-3J_t}}{28} \sum_{j_x=J_x+1}^{\infty} 2^{-4j_x},$$

$$\sum_{r=1}^{\kappa} \|u_r(x,t) - P_{V_2^{J_x,J_t}} u_r(x,t)\|_{L^2(0,l_r)} \leq \Theta_1 2^{-4J_x-3J_t}, \tag{57}$$

where Θ_1 is a constant given by $\Theta_1 = \frac{3\kappa\Re\mathtt{A}^2}{420}$.

Lemma 3 *Let $u_r(x,t)$ be the accurate solution of NDDE-MSG (1) and $P_{V_2^{J_x,J_t}} u_r(x,t)$ be the projection of analytic solution such that $|\partial_{tt}\partial_{xxx} u_r(x,t)| \leq \Re_r$, $\forall\ (x,t) \in (0,1)\times(0,1)$ and $\Re_r > 0, r = 1(1)\kappa$ and $\partial_t\partial_{xx} u_r(x,t) = \sum_{i_x=1}^{\infty}\sum_{i_t=1}^{\infty} g^r_{i_x,i_t}\psi_{i_x}(x)\psi_{i_t}(t)$, then the following inequality holds:*

$$\sum_{r=1}^{\kappa} \|u_r(x,t-\tau_r) - P_{V_2^{J_x,J_t}} u_r(x,t-\tau_r)\|_{L^2(0,l_r)} \leq \Theta_1 2^{-4J_x-3J_t}. \tag{58}$$

Proof Similar techniques to those used in proving Lemma 2 can be employed in establishing the proof of this lemma.

Lemma 4 *Let $u_r(x,t)$ be the accurate solution of NDDE-MSG (1) and $P_{V_2^{J_x,J_t}} u_r(x,t)$ be the projection of analytic solution such that $|\partial_{tt}\partial_{xxx} u_r(x,t)| \leq \Re_r$, $\forall\ (x,t) \in (0,1)\times(0,1)$ and $\Re_r > 0, r = 1(1)\kappa$ and $\partial_t\partial_{xx} u_r(x,t) = \sum_{i_x=1}^{\infty}\sum_{i_t=1}^{\infty} g^r_{i_x,i_t}\psi_{i_x}(x)\psi_{i_t}(t)$, then the following inequality holds:*

$$\sum_{r=1}^{\kappa} \|\partial_x u_r(x,t) - P_{V_2^{J_x,J_t}} \partial_x u_r(x,t)\|_{L^2(0,l_r)} \leq 2^{-3J_t}\big(\Theta_2 2^{-3J_x} + \Theta_3 2^{-4J_x}\big), \tag{59}$$

where Θ_2 and Θ_3 are constants given in the proof below.

Proof From equation (53), we have

$$\sum_{r=1}^{\kappa} \|\partial_x u_r(x,t) - P_{V_2^{J_x,J_t}} \partial_x u_r(x,t)\|_{L^2(0,l_r)} = \sum_{r=1}^{\kappa} \Big\| \mathop{\Omega}_{j_x,i_x,j_t,i_t} g^r_{i_x,i_t}(\mathfrak{I}^{(1)}_x \psi_{i_x}(x)\mathfrak{I}^{(1)}_t \psi_{i_t}(t) - \mathfrak{I}^{(2)}_x \psi_{i_x}(1)\mathfrak{I}^{(1)}_t \psi_{i_t}(t))$$
$$+ \frac{1}{\kappa} \mathop{\Omega}_{j_x,i_x,j_t,i_t} \sum_{r=1}^{\kappa} g^r_{i_x,i_t}\mathfrak{I}^{(2)}_x \psi_{i_x}(1)\mathfrak{I}^{(1)}_t \psi_{i_t}(t)\Big\|_{L^2(0,l_r)}. \tag{60}$$

Using Minkowski and Hölder inequalities, we have

$$\sum_{r=1}^{\kappa} \|\partial_x u_r(x,t) - P_{V_2^{J_x,J_t}} \partial_x u_r(x,t)\|_{L^2(0,l_r)} \leq \sum_{r=1}^{\kappa} \mathop{\Omega}_{j_x,i_x,j_t,i_t} |g^r_{i_x,i_t}| \Bigg(\bigg(\int_0^1 |\mathfrak{I}^{(1)}_x \psi_{i_x}(x)|^2 dx \bigg)^{\frac{1}{2}} \bigg(\int_0^1 |\mathfrak{I}^{(1)}_t \psi_{i_t}(t)|^2 dt \bigg)^{\frac{1}{2}}$$
$$+ \bigg(\int_0^1 |\mathfrak{I}^{(2)}_x \psi_{i_x}(1)|^2 dx \bigg)^{\frac{1}{2}} \bigg(\int_0^1 |\mathfrak{I}^{(1)}_t \psi_{i_t}(t)|^2 dt \bigg)^{\frac{1}{2}}$$
$$+ \bigg(\int_0^1 |\mathfrak{I}^{(2)}_x \psi_{i_x}(1)|^2 dx \bigg)^{\frac{1}{2}} \Big(\int_0^1 |\mathfrak{I}^{(1)}_t \psi_{i_t}(t)|^2 dt \Big)^{\frac{1}{2}} \Bigg). \tag{61}$$

Now from equations (55), (56) and (61), we obtain

$$\sum_{r=1}^{\kappa} \|\partial_x u_r(x,t) - P_{V_2^{J_x,J_t}} \partial_x u_r(x,t)\|_{L^2(0,l_r)} \leq \mathop{\Omega}_{j_x,i_x,j_t,i_t} \frac{\Re\kappa\mathtt{A}^2}{4} \Big(2^{-4j_x} + 2^{-5j_x+1} \Big) 2^{-4j_t}$$
$$= \frac{\Re\kappa\mathtt{A}^2}{4} \sum_{j_x=J_x+1}^{\infty} \sum_{i_x=2^{j_x}}^{2^{j_x+1}-1} \Big(2^{-4j_x} + 2^{-5j_x+1} \Big) \sum_{j_t=J_t+1}^{\infty} 2^{-3j_t}$$

$$= \frac{2^{-3J_t}\Re\kappa\mathtt{A}^2}{28}\sum_{j_x=J_x+1}^{\infty}\left(2^{-3j_x}+2^{-4j_x+1}\right),$$

$$\sum_{r=1}^{\kappa}\|\partial_x u_r(x,t)-P_{V_2^{J_x,J_t}}\partial_x u_r(x,t)\|_{L^2(0,l_r)} \le 2^{-3J_t}\left(\Theta_2 2^{-3J_x}+\Theta_3 2^{-4J_x}\right), \tag{62}$$

where Θ_2 and Θ_3 are constants given by $\Theta_2 = \frac{\Re\kappa\mathtt{A}^2}{196}$, $\Theta_3 = \frac{\Re\kappa\mathtt{A}^2}{210}$.

Lemma 5 *Let $u_r(x,t)$ be the accurate solution of NDDE-MSG (1) and $P_{V_2^{J_x,J_t}}u_r(x,t)$ be the projection of analytic solution such that $|\partial_{tt}\partial_{xxx}u_r(x,t)| \le \Re_r$, $\forall (x,t)\in(0,1)\times(0,1)$ and $\Re_r > 0, r = 1(1)\kappa$ and $\partial_t\partial_{xx}u_r(x,t) = \sum_{i_x=1}^{\infty}\sum_{i_t=1}^{\infty} g^r_{i_x,i_t}\psi_{i_x}(x)\psi_{i_t}(t)$, then the following inequality holds:*

$$\sum_{r=1}^{\kappa}\|\partial_x u_r(x,t-\tau_{1,r})-P_{V_2^{J_x,J_t}}\partial_x u_r(x,t-\tau_{1,r})\|_{L^2(0,l_r)} \le 2^{-3J_t}\left(\Theta_2 2^{-3J_x}+\Theta_3 2^{-4J_x}\right). \tag{63}$$

Proof Similar techniques to those used in proving Lemma 4 can be employed in establishing the proof of this lemma.

Lemma 6 *Let $u_r(x,t)$ be the accurate solution of NDDE-MSG (1) and $P_{V_2^{J_x,J_t}}u_r(x,t)$ be the projection of analytic solution such that $|\partial_{tt}\partial_{xxx}u_r(x,t)| \le \Re_r$, $\forall (x,t)\in(0,1)\times(0,1)$ and $\Re_r > 0, r = 1(1)\kappa$ and $\partial_t\partial_{xx}u_r(x,t) = \sum_{i_x=1}^{\infty}\sum_{i_t=1}^{\infty} g^r_{i_x,i_t}\psi_{i_x}(x)\psi_{i_t}(t)$, then the following inequality holds:*

$$\sum_{r=1}^{\kappa}\|\partial_{xx}u_r(x,t)-P_{V_2^{J_x,J_t}}\partial_{xx}u_r(x,t)\|_{L^2(0,l_r)} \le \Theta_4 2^{-J_x-3J_t}, \tag{64}$$

where Θ_4 is a constant given in the proof below.

Proof From equation (53), we have

$$\sum_{r=1}^{\kappa}\left\|\partial_{xx}u_r(x,t)-P_{V_2^{J_x,J_t}}\partial_{xx}u_r(x,t)\right\|_{L^2(0,l_r)} = \sum_{r=1}^{\kappa}\left\|\Omega_{j_x,i_x,j_t,i_t} g^r_{i_x,i_t}\psi_{i_x}(x)\mathcal{I}_t^{(1)}\psi_{i_t}(t)\right\|_{L^2(0,l_r)}. \tag{65}$$

Using Hölder inequality, we have

$$\sum_{r=1}^{\kappa}\left\|\partial_{xx}u_r(x,t)-P_{V_2^{J_x,J_t}}\partial_{xx}u_r(x,t)\right\|_{L^2(0,l_r)} \le \sum_{r=1}^{\kappa}\Omega_{j_x,i_x,j_t,i_t}|g^r_{i_x,i_t}|\left(\int_0^1|\psi_{i_x}(x)|^2dx\right)^{\frac{1}{2}}\left(\int_0^1|\mathcal{I}_t^{(1)}\psi_{i_t}(t)|^2dt\right)^{\frac{1}{2}}. \tag{66}$$

Using equations (56), we have

$$\begin{aligned}\sum_{r=1}^{\kappa}\|\partial_{xx}u_r(x,t)-P_{V_2^{J_x,J_t}}\partial_{xx}u_r(x,t)\|_{L^2(0,l_r)} &\le \Omega_{j_x,i_x,j_t,i_t}\frac{\Re\kappa\mathtt{A}}{4}2^{-2j_x-4j_t}\\ &= \frac{\Re\kappa\mathtt{A}}{4}\sum_{j_x=J_x+1}^{\infty}\sum_{i_x=2^{j_x}}^{2^{j_x+1}-1}2^{-2j_x}\sum_{j_t=J_t+1}^{\infty}2^{-3j_t}\\ &= \frac{2^{-3J_t}\Re\kappa\mathtt{A}}{28}\sum_{j_x=J_x+1}^{\infty}2^{-j_x},\end{aligned}$$

$$\sum_{r=1}^{\kappa}\|\partial_{xx}u_r(x,t)-P_{V_2^{J_x,J_t}}\partial_{xx}u_r(x,t)\|_{L^2(0,l_r)} \le \Theta_4 2^{-J_x-3J_t}, \tag{67}$$

where $\Theta_4 = \frac{\Re\kappa\mathtt{A}}{28}$.

Lemma 7 *Let $u_r(x,t)$ be the accurate solution of NDDE-MSG (1) and $P_{V_2^{J_x,J_t}}u_r(x,t)$ be the projection of analytic solution such that $|\partial_{tt}\partial_{xxx}u_r(x,t)| \leq \Re_r$, $\forall (x,t) \in (0,1)\times(0,1)$ and $\Re_r > 0, r = 1(1)\kappa$ and $\partial_t\partial_{xx}u_r(x,t) = \sum_{i_x=1}^{\infty}\sum_{i_t=1}^{\infty} g^r_{i_x,i_t}\psi_{i_x}(x)\psi_{i_t}(t)$, then the following inequality holds:*

$$\sum_{r=1}^{\kappa}\left\|\partial_{xx}u_r(x,t-\tau_{2,r}) - P_{V_2^{J_x,J_t}}\partial_{xx}u_r(x,t-\tau_{2,r})\right\|_{L^2(0,l_r)} \leq \Theta_4 2^{-J_x-3J_t}. \tag{68}$$

Proof Similar techniques to those used in proving Lemma 6 can be employed in establishing the proof of this lemma.

Lemma 8 *Let $u_r(x,t)$ be the accurate solution of NDDE-MSG (1) and $P_{V_2^{J_x,J_t}}u_r(x,t)$ be the projection of analytic solution such that $|\partial_{tt}\partial_{xxx}u_r(x,t)| \leq \Re_r$, $\forall (x,t) \in (0,1)\times(0,1)$ and $\Re_r > 0, r = 1(1)\kappa$ and $\partial_t\partial_{xx}u_r(x,t) = \sum_{i_x=1}^{\infty}\sum_{i_t=1}^{\infty} g^r_{i_x,i_t}\psi_{i_x}(x)\psi_{i_t}(t)$, then the following inequality holds:*

$$\sum_{r=1}^{\kappa}\left\|\left(\partial_t u_r(x,t) - P_{V_2^{J_x,J_t}}\partial_t u_r(x,t)\right)\right\|_{L^2(0,l_r)} \leq \Theta_5 2^{-4J_x-J_t}, \tag{69}$$

where θ_5 is a constant given in the proof below.

Proof From equation (53), we have

$$\begin{aligned}\sum_{r=1}^{\kappa}\left\|\left(\partial_t u_r(x,t) - P_{V_2^{J_x,J_t}}\partial_t u_r(x,t)\right)\right\|_{L^2(0,l_r)} &= \sum_{r=1}^{\kappa}\Big\|\underset{j_x,i_x,j_t,i_t}{\Omega} g^r_{i_x,i_t}(\mathcal{I}_x^{(2)}\psi_{i_x}(x)\psi_{i_t}(t) - x\mathcal{I}_x^{(2)}\psi_{i_x}(1))\psi_{i_t}(t)\\ &\quad - \frac{1}{\kappa}\underset{j_x,i_x,j_t,i_t}{\Omega}\sum_{r=1}^{\kappa} g^r_{i_x,i_t}(1-x)\mathcal{I}_x^{(2)}\psi_{i_x}(1)\psi_{i_t}(t)\Big\|_{L^2(0,l_r)}.\end{aligned} \tag{70}$$

Using Minkowski and Hölder inequalities, we have

$$\begin{aligned}\sum_{r=1}^{\kappa}\|\partial_t u_r(x,t) - P_{V_2^{J_x,J_t}}\partial_t u_r(x,t)\|_{L^2(0,l_r)} &\leq \sum_{r=1}^{\kappa}\underset{j_x,i_x,j_t,i_t}{\Omega}|g^r_{i_x,i_t}|\Bigg(\left(\int_0^1|\mathcal{I}_x^{(2)}\psi_{i_x}(x)|^2dx\right)^{\frac{1}{2}}\left(\int_0^1|\psi_{i_t}(t)|^2dt\right)^{\frac{1}{2}}\\ &\quad + \left(\int_0^1|x\mathcal{I}_x^{(2)}\psi_{i_x}(1)|^2dx\right)^{\frac{1}{2}}\left(\int_0^1|\psi_{i_t}(t)|^2dt\right)^{\frac{1}{2}}\\ &\quad + \left(\int_0^1|(1-x)\mathcal{I}_x^{(2)}\psi_{i_x}(1)|^2dx\right)^{\frac{1}{2}}\left(\int_0^1|\psi_{i_t}(t)|^2dt\right)^{\frac{1}{2}}\Bigg).\end{aligned} \tag{71}$$

Using equation (56), we obtain

$$\begin{aligned}\sum_{r=1}^{\kappa}\|\partial_t u_r(x,t) - P_{V_2^{J_x,J_t}}\partial_t u_r(x,t)\|_{L^2(0,l_r)} &\leq \underset{j_x,i_x,j_t,i_t}{\Omega}\frac{3\kappa\Re\mathtt{A}}{4}2^{-5j_x-2j_t}\\ &= \frac{3\kappa\Re\mathtt{A}}{4}\sum_{j_x=J_x+1}^{\infty}\sum_{i_x=2^{j_x}}^{2^{j_x+1}-1}2^{-5j_x}\sum_{j_t=J_t+1}^{\infty}2^{-j_t}\\ &= \frac{2^{-J_t}3\kappa\Re\mathtt{A}}{4}\sum_{j_x=J_x+1}^{\infty}2^{-4j_x},\end{aligned}$$

$$\sum_{r=1}^{\kappa}\|\partial_t u_r(x,t) - P_{V_2^{J_x,J_t}}\partial_t u_r(x,t)\|_{L^2(0,l_r)} \leq \Theta_5 2^{-4J_x-J_t}, \tag{72}$$

where $\Theta_5 = \frac{\kappa\Re\mathtt{A}}{20}$.

Theorem 1 *Let* $u_r(x,t)(=\{u_r(x,t)\}_{r=1}^{\kappa}) \in C\left(\overline{\mathcal{G}(\mathcal{V},\mathcal{E})} \times \left[t_0 - \tau_r\left(x,t,u_r(x,t)\right), t_f\right]; \mathbb{R}\right)$ *be the exact solution of NDDE-MSG (1) and* $P_{V_2^{J_x,J_t}} u_r(x,t)$ *be the approximate solution such that* $|\partial_{tt}\partial_{xxx}u_r(x,t)| \leq \Re_r, \forall (x,t) \in (0,1)\times(0,1)$ *and* $\Re_r > 0, r = 1(1)\kappa$ *and* $\partial_t\partial_{xx}u_r(x,t) = \sum_{i_x=1}^{\infty}\sum_{i_t=1}^{\infty} g_{i_x,i_t}^r \psi_{i_x}(x)\psi_{i_t}(t)$. *Let* F_r *in equation (1) be the Lipschitz function with Lipschitz coefficients* $\mathscr{L}_{i,r},\ i = 1,2,...,6$. *If we denote* ε_{J_x,J_t}^r *as the obtained error associated with the* r^{th} *edge, then the global error associated with the graph is denoted by* $\varepsilon_{J_xJ_t}^{\mathcal{G}(\mathcal{V},\mathcal{E})} = \sum_{r=1}^{\kappa} \|\varepsilon_{J_x,J_t}^r\|_{L^2(0,l_r)}$ *and estimated by the following inequality:*

$$\varepsilon_{J_xJ_t}^{\mathcal{G}(\mathcal{V},\mathcal{E})} = \sum_{r=1}^{\kappa} \|\varepsilon_{J_x,J_t}^r\|_{L^2(0,l_r)} \leq \mathcal{C}_1 2^{-4J_x-J_t} + (\mathcal{C}_2 2^{-4J_x} + \mathcal{C}_3 2^{-3J_x} + \mathcal{C}_4 2^{-2J_x})2^{-3J_t}, \tag{73}$$

where $\mathcal{C}_1,\ \mathcal{C}_2,\ \mathcal{C}_3$ *and* $\mathcal{C}_4$ *are constants given in the proof below.*

Proof We have

$$\begin{aligned}
\sum_{r=1}^{\kappa} \left\|\varepsilon_{J_x,J_t}^r\right\|_{L^2(0,l_r)} = \sum_{r=1}^{\kappa} \Big\| & \partial_t u_r(x,t) - F_r(x,t,u_r,u_r(x,t-\tau_r),\partial_x u_r(x,t),\partial_x u_r\left(x,t-\tau_{1,r}\right),\partial_{xx}u_r(x,t),\\
& \partial_{xx}u_r\left(x,t-\tau_{2,r}\right)) - P_{V_2^{J_x,J_t}}\partial_t u_r(x,t) + F_r\big(x,t,P_{V_2^{J_x,J_t}}u_r,P_{V_2^{J_x,J_t}}u_r\left(x,t-\tau_r\right),P_{V_2^{J_x,J_t}}\partial_x u_r(x,t),\\
& P_{V_2^{J_x,J_t}}\partial_x u_r\left(x,t-\tau_{1,r}\right),P_{V_2^{J_x,J_t}}\partial_{xx}u_r(x,t),P_{V_2^{J_x,J_t}}\partial_{xx}u_r\left(x,t-\tau_{2,r}\right)\big)\Big\|_{L^2(0,l_r)}\\
\leq \sum_{r=1}^{\kappa} \big(& \|\partial_t u_r(x,t) - P_{V_2^{J_x,J_t}}\partial_t u_r(x,t)\|_{L^2(0,l_r)} + \mathscr{L}_{1,r}\|u_r(x,t) - P_{V_2^{J_x,J_t}}u_r(x,t)\|_{L^2(0,l_r)}\\
& + \mathscr{L}_{2,r}\|u_r(x,t-\tau_r) - P_{V_2^{J_x,J_t}}u_r(x,t-\tau_r)\|_{L^2(0,l_r)} + \mathscr{L}_{3,r}\|\partial_x u_r(x,t) - P_{V_2^{J_x,J_t}}\partial_x u_r(x,t)\|_{L^2(0,l_r)}\\
& + \mathscr{L}_{4,r}\|\partial_x u_r(x,t-\tau_{1,r}) - P_{V_2^{J_x,J_t}}\partial_x u_r(x,t-\tau_{1,r})\|_{L^2(0,l_r)} + \mathscr{L}_{5,r}\|\partial_{xx}u_r(x,t) - P_{V_2^{J_x,J_t}}\partial_{xx}u_r(x,t)\|_{L^2(0,l_r)}\\
& + \mathscr{L}_{6,r}\|\partial_{xx}u_r(x,t-\tau_{2,r}) - P_{V_2^{J_x,J_t}}\partial_{xx}u_r(x,t-\tau_{2,r})\|_{L^2(0,l_r)}\big).
\end{aligned} \tag{74}$$

Using Lemmas 1-8 in equation (74) provides

$$\sum_{r=1}^{\kappa} \|\varepsilon_{J_x,J_t}^r\|_{L^2(0,l_r)} \leq \mathcal{C}_1 2^{-4J_x-J_t} + (\mathcal{C}_2 2^{-4J_x} + \mathcal{C}_3 2^{-3J_x} + \mathcal{C}_4 2^{-2J_x})2^{-3J_t}, \tag{75}$$

where $\mathcal{C}_1 = \kappa\Theta_5,\ \mathcal{C}_2 = (\mathscr{L}_1+\mathscr{L}_2)\Theta_1 + (\mathscr{L}_3+\mathscr{L}_4)\Theta_3,\ \mathcal{C}_3 = (\mathscr{L}_3+\mathscr{L}_4)\Theta_2$ and $\mathcal{C}_4 = (\mathscr{L}_5+\mathscr{L}_6)\Theta_4$, $\mathscr{L}_i = \max_{1\leq r\leq\kappa} \mathscr{L}_{i,r},\ i = 1,2,...,6$. From equation (75), it is obvious that the error is inversely proportional to the resolution levels J_x and J_t. Hence, if J_x and J_t tend to ∞, the global error goes to zero. This completes the proof.

7 Numerical examples

This section presents five examples of NDDE-MSG using the Haar wavelet approach. Calculations were performed using MATLAB R2021a, an AMD Ryzen 5 PRO 5650U processor, and Windows 11. The following error norms are computed for numerical results:

$$\varepsilon_{J_x,J_t}^{r,\infty} = \max_{i_x,i_t} \left| u_r(x,t) - P_{V_2^{J_x,J_t}}u_r(x,t)\right|,\ r = 1(1)\kappa, \tag{76}$$

$$\varepsilon_{J_x,J_t}^{r,2} = \left\| u_r(x,t) - P_{V_2^{J_x,J_t}}u_r(x,t)\right\|_{L^2(0,l_r)},\ r = 1(1)\kappa. \tag{77}$$

Example 1 Consider the following linear NDDE-MSG (1) with three edges:

$$\begin{gathered}\partial_t u_r(x,t) = \partial_{xx} u_r(x,t-\sqrt{t}) + u_r(x,t-\sin(t)) + f_r(x,t), \quad x \in (0,1), t \in (0,1), \\ u_r(x,t) = 0, \quad t \le 0, \\ u_r(0,t) = u_s(0,t), \quad r \ne s, r = 1,2,3, \ s = 1,2,3, \\ \sum_{r=1}^{3} \partial_x u_r(0,t) = 0, \\ u_r(1,t) = 0, \ 1 \le r \le 3. \end{gathered} \tag{78}$$

The analytical solutions of this example are $u_1(x,t) = u_2(x,t) = t^2 \sin(\pi x)$, $u_3(x,t) = -2t^2 \sin(\pi x)$ and the source functions $f_r(x,t)$, $r = 1,2,3$ can be calculated with the assistance of the exact solutions. The obtained maximum absolute errors (MAEs) ($\varepsilon^{r,\infty}_{J_x,J_t}$, $r = 1,2,3$) and root mean square errors (RMSEs) ($\varepsilon^{r,2}_{J_x,J_t}$, $r = 1,2,3$) are tabulated in Table 1. The table shows that as the values of the resolution parameters J_x, J_t are increased, the absolute errors (AEs) decrease significantly, which is a good support of Theorem 1. The graphs of approximate solutions $P_{V_2^{J_x,J_t}} u_r(x,t_{N_t})$, $r = 1,2,3$ are given in Figure 2a. The accurate and approximate solutions of $u_1(x,t_{N_t})$ are compared in Figure 2b, which demonstrates that the approximate and exact solutions are similar. In addition, the influence of the resolution parameters J_x, J_t on the behaviour of AEs are illustrated in Figure 3. According to the figures, the AEs for $J_x = J_t = 4$ are $O(e-03)$, but for $J_x = J_t = 5$, they are $O(e-04)$, which is in good accordance with the theoretical results.

Table 1: Effect of J_x, J_t on the obtained MAEs and RMSEs of Example 1.

$J_x = J_t$	$\varepsilon^{1,\infty}_{J_x,J_t} = \varepsilon^{2,\infty}_{J_x,J_t}$	$\varepsilon^{3,\infty}_{J_x,J_t}$	CPU	$\varepsilon^{1,2}_{J_x,J_t} = \varepsilon^{2,2}_{J_x,J_t}$	$\varepsilon^{3,2}_{J_x,J_t}$	CPU
1	$3.9580e-02$	$7.9161e-02$	0.04	$8.0851e-02$	$1.6170e-01$	0.03
2	$1.2404e-02$	$2.4808e-02$	0.04	$4.6820e-02$	$9.3641e-02$	0.04
3	$3.4796e-03$	$6.9592e-03$	0.40	$2.5690e-02$	$5.1381e-02$	0.05
4	$8.9695e-04$	$1.7939e-03$	1.06	$1.3131e-02$	$2.6262e-02$	0.41
5	$2.2871e-04$	$4.5742e-04$	6.48	$6.6772e-03$	$1.3354e-02$	6.47

Example 2 Consider the following linear NDDE-MSG (1) with three edges:

$$\begin{gathered}\partial_t u_r(x,t) = \partial_{xx} u_r(x,t) + \partial_x u_r(x,\sin(\sqrt{t})) + f_r(x,t), \quad x \in (0,1), t \in (0,1), \\ u_1(x,t) = u_2(x,t) = \sin(2\pi x), \ u_3(x,t) = -2\sin(2\pi x), \quad t \le 0, \\ u_r(0,t) = u_s(0,t), \quad r \ne s, r = 1,2,3, \ s = 1,2,3, \\ \sum_{r=1}^{3} \partial_x u_r(0,t) = 0, \\ u_r(1,t) = 0, \ 1 \le r \le 3. \end{gathered} \tag{79}$$

The analytical solutions of this example are $u_1(x,t) = u_2(x,t) = t^3 \sin(2\pi x) + \sin(2\pi x)$,
$u_3(x,t) = -2t^3 \sin(2\pi x) - 2\sin(2\pi x)$ and the source functions $f_r(x,t)$, $r = 1,2,3$ can be calculated with the assistance of the exact solutions. The obtained MAEs ($\varepsilon^{r,\infty}_{J_x,J_t}$, $r = 1,2,3$) and RMSEs ($\varepsilon^{r,2}_{J_x,J_t}$, $r = 1,2,3$) are tabulated in Table 2. The table shows that as the values of the resolution parameters J_x, J_t are increased, the AEs decrease significantly, which is a good support of the Theorem 1. The graphs of approximate solutions $P_{V_2^{J_x,J_t}} u_r(x,t_{N_t})$, $r = 1,2,3$ are given in Figure 4a. Figure 4b compares the accurate

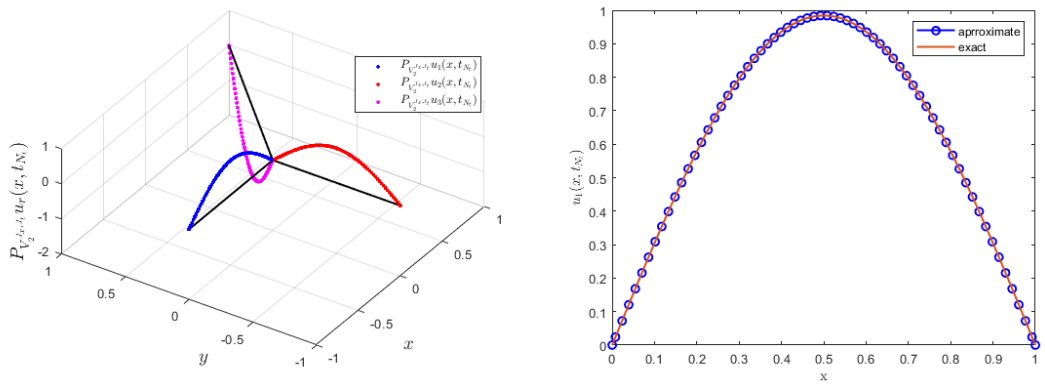

(a) (b)

Fig. 2: (2a) Graph of $P_{V_2^{J_x,J_t}} u_r(x,t)$, $r = 1,2,3$ of Example 1 at $t = t_{N_t}$ for $J_x = J_t = 5$. (2b) Graphical comparison of analytic and approximate solutions of $u_1(x,t)$ at $t = t_{N_t}$ for $J_x = J_t = 5$

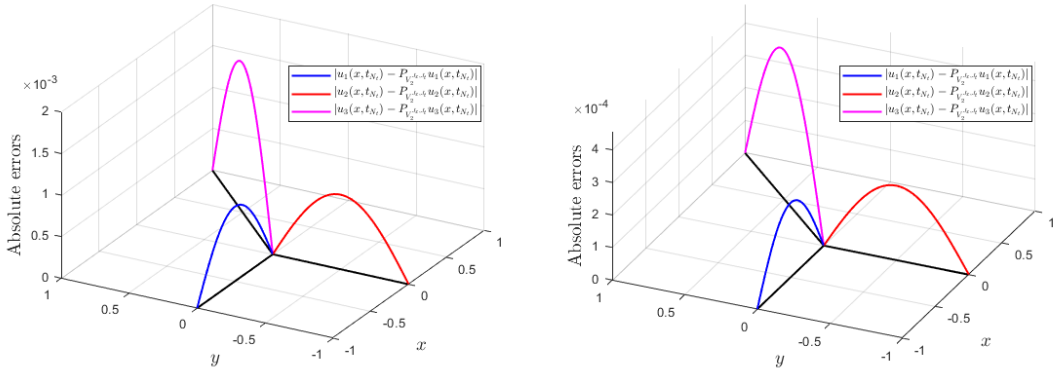

(a) (b)

Fig. 3: Impact of resolution parameters J_x, J_t on AEs obtained for $u(x,t)$ of Example 1 at $t = t_{N_t}$: (3a) for $J_x = J_t = 4$, (3b) for $J_x = J_t = 5$

and approximate solutions of $u_2(x,t_{N_t})$, demonstrating that the approximate solution is similar to the exact solution. In addition, Figure 5 illustrates the influence of the resolution parameters J_x, J_t on the behaviour of AEs. According to the figures, the AEs for $J_x = J_t = 3$ are $O(e-02)$, but the AEs for $J_x = J_t = 4$ are $O(e-03)$, which is in good accordance with the theoretical results.

Example 3 Consider the following linear NDDE-MSG (1) with four edges:

$$\partial_t u_r(x,t) = \partial_{xx} u_r(x,t) - u_r(x,\sqrt{sin(t)}) + f_r(x,t), \quad x \in (0,1), t \in (0,1), \ 1 \le r \le 4,$$
$$u_r(x,t) = 0, \quad t \le 0,$$
$$u_r(0,t) = u_s(0,t), \quad r \ne s, r = 1,2,3,4, \ s = 1,2,3,4,$$
$$\sum_{r=1}^{4} \partial_x u_r(0,t) = 0,$$

Table 2: Effect of J_x, J_t on the obtained MAEs and RMSEs of Example 2

$J_x = J_t$	$\varepsilon^{1,\infty}_{J_x,J_t} = \varepsilon^{2,\infty}_{J_x,J_t}$	$\varepsilon^{3,\infty}_{J_x,J_t}$	CPU	$\varepsilon^{1,2}_{J_x,J_t} = \varepsilon^{2,2}_{J_x,J_t}$	$\varepsilon^{3,2}_{J_x,J_t}$	CPU
1	$5.6551e-02$	$1.1310e-01$	0.06	$7.8003e-02$	$1.5600e-01$	0.04
2	$2.1736e-02$	$4.3472e-02$	0.05	$4.9131e-02$	$9.8262e-02$	0.05
3	$6.3922e-03$	$1.2784e-02$	0.09	$2.6085e-02$	$5.2170e-02$	0.08
4	$1.6580e-03$	$3.3160e-03$	1.20	$1.3131e-02$	$2.6262e-02$	1.29
5	$4.2724e-04$	$8.5449e-04$	52.97	$6.5944e-03$	$1.3188e-02$	53.30

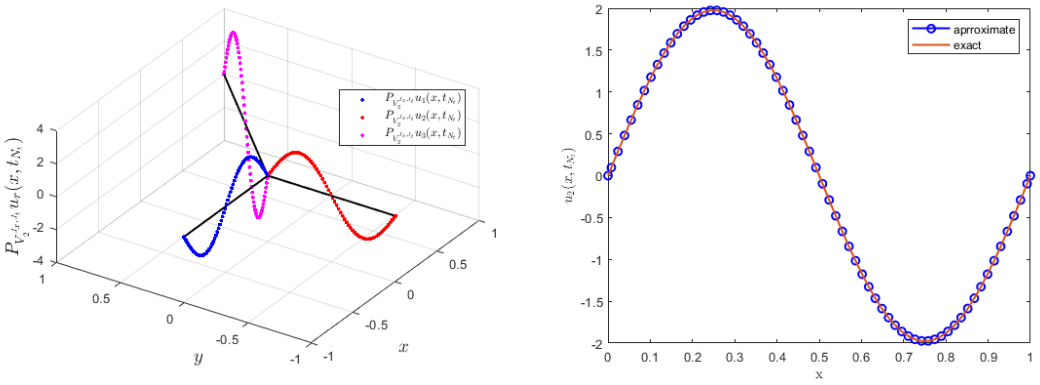

(a) (b)

Fig. 4: (4a) Graph of $P_{V_2^{J_x,J_t}} u_r(x,t)$, $r = 1,2,3$ of Example 2 at $t = t_{N_t}$ for $J_x = J_t = 5$. (4b) Comparison of exact and approximate solution of $u_2(x,t)$ at $t = t_{N_t}$ for $J_x = J_t = 5$

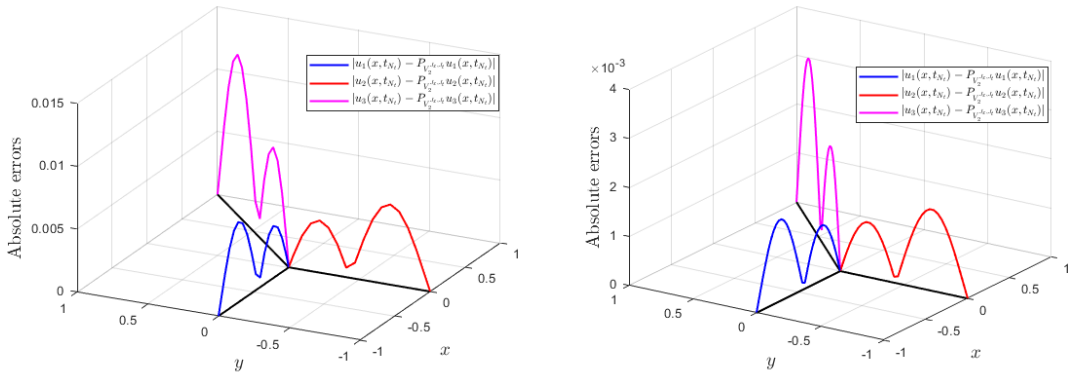

(a) (b)

Fig. 5: Impact of resolution parameters J_x, J_t on AEs obtained for $u(x,t)$ of Example 2 at $t = t_{N_t}$: (5a) for $J_x = J_t = 3$, (5b) for $J_x = J_t = 4$

$$u_r(1,t)=0,\ 1\le r\le 4. \tag{80}$$

The analytical solutions of this example are $u_1(x,t)=u_2(x,t)=t^2x(1-x)$, $u_3(x,t)=u_4(x,t)=-t^2x(1-x)$ and the source functions $f_r(x,t)$, $r=1,2,3,4$ can be calculated with the assistance of the exact solutions. The obtained MAEs ($\varepsilon^{r,\infty}_{J_x,J_t}$, $r=1,2,3,4$) and RMSEs ($\varepsilon^{r,2}_{J_x,J_t}$, $r=1,2,3,4$) are tabulated in Table 3. The table shows that when the values of the resolution parameters J_x, J_t are increased, the MAEs and RMSEs decrease gradually, which is a good support of Theorem 1.

Table 3: Effect of J_x, J_t on the obtained MAEs and RMSEs of Example 3.

$J_x=J_t$	$\varepsilon^{1,\infty}_{J_x,J_t}=\varepsilon^{2,\infty}_{J_x,J_t}$	$\varepsilon^{3,\infty}_{J_x,J_t}=\varepsilon^{4,\infty}_{J_x,J_t}$	CPU	$\varepsilon^{1,2}_{J_x,J_t}=\varepsilon^{2,2}_{J_x,J_t}$	$\varepsilon^{3,2}_{J_x,J_t}=\varepsilon^{4,2}_{J_x,J_t}$	CPU
1	$1.6603e-03$	$1.6603e-03$	0.04	$2.5831e-03$	$2.5831e-03$	0.03
2	$6.4079e-04$	$6.4079e-04$	0.04	$1.3779e-03$	$1.3779e-03$	0.04
3	$1.9078e-04$	$1.9078e-04$	0.06	$6.6389e-04$	$6.6389e-04$	0.07
4	$5.4193e-05$	$5.4193e-05$	0.60	$3.3886e-04$	$3.3886e-04$	0.58
5	$1.4269e-05$	$1.4269e-05$	14.89	$1.6473e-04$	$1.6473e-04$	15.22

Example 4 Consider the following nonlinear NDDE-MSG (1) with three edges:

$$\begin{gathered}\partial_t u_r(x,t)=\partial_{xx}u_r(x,\sin t)+u_r^2+f_r(x,t),\quad x\in(0,1),t\in(0,1),\ 1\le r\le 3,\\ u_r(x,t)=0,\quad t\le 0,\\ u_r(0,t)=u_s(0,t),\quad r\ne s,r=1,2,3,\ \ s=1,2,3,\\ \sum_{r=1}^{3}\partial_x u_r(0,t)=0,\\ u_r(1,t)=0,\ 1\le r\le 3.\end{gathered} \tag{81}$$

The analytical solutions of this example are $u_1(x,t)=u_2(x,t)=t^2\sin(2\pi x)$, $u_3(x,t)=-2t^2\sin(2\pi x)$ and the source functions $f_r(x,t)$, $r=1,2,3$ can be calculated with the assistance of the exact solutions. The obtained MAEs ($\varepsilon^{r,\infty}_{J_x,J_t}$, $r=1,2,3$) and RMSEs ($\varepsilon^{r,2}_{J_x,J_t}$, $r=1,2,3$) are tabulated in Table 4. The table shows that as the values of the resolution parameters J_x, J_t are increased, the MAEs and RMSEs decrease significantly, which is a good support of Theorem 1. The graphs of approximate solutions $P_{V_2^{J_x,J_t}}u_r(x,t_{N_t})$, $r=1,2,3$ are given in Figure 6a. Figure 6b compares the accurate and approximate solutions of $u_2(x,t_{N_t})$, demonstrating that the approximate solution is similar to the exact solution. In addition, Figure 7 illustrates the effect of the resolution parameters J_x, J_t on the behaviour of AEs. According to the Figures, the AEs for $J_x=J_t=4$ are $O(e-02)$, but the AEs for $J_x=J_t=5$ are $O(e-03)$, which is in good accordance with the theoretical results.

Example 5 Consider the following linear NDDE-MSG (1) with three edges:

$$\begin{gathered}\partial_t u_r(x,t)=\partial_{xx}u_r(x,t)+u_r(x,\sqrt{\sin t})+f_r(x,t),\quad x\in(0,2),t\in(0,2),\\ u_r(x,t)=0,\quad t\le 0,\\ u_r(0,t)=u_s(0,t),\quad r\ne s,r=1,2,3,\ \ s=1,2,3,\\ \sum_{r=1}^{3}\partial_x u_r(0,t)=0,\\ u_r(2,t)=0,\ 1\le r\le 3.\end{gathered} \tag{82}$$

Table 4: Effect of J_x, J_t on the obtained MAEs and RMSEs of Example 4.

$J_x = J_t$	$\varepsilon^{1,\infty}_{J_x,J_t} = \varepsilon^{2,\infty}_{J_x,J_t}$	$\varepsilon^{3,\infty}_{J_x,J_t}$	CPU	$\varepsilon^{1,2}_{J_x,J_t} = \varepsilon^{2,2}_{J_x,J_t}$	$\varepsilon^{3,2}_{J_x,J_t}$	CPU
1	$1.5039e-01$	$7.9161e-01$	0.07	$2.7422e-01$	$5.9493e-01$	0.07
2	$7.7248e-02$	$2.1235e-01$	0.09	$1.8332e-01$	$4.2204e-01$	0.13
3	$2.5588e-02$	$7.7248e-02$	0.37	$1.0573e-01$	$2.4800e-01$	0.49
4	$7.3959e-03$	$2.3482e-02$	10.64	$5.8825e-02$	$1.3936e-01$	11.41

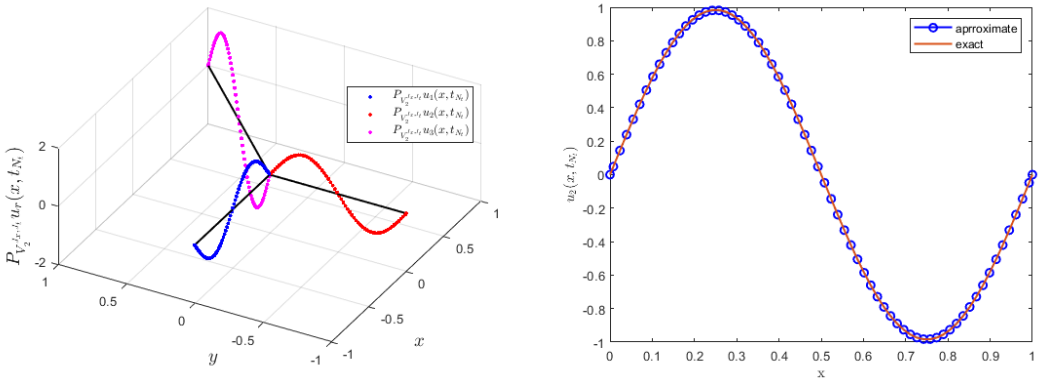

(a) (b)

Fig. 6: (6a) Graph of $P_{V_2^{J_x,J_t}} u_r(x,t)$, $r = 1,2,3$ of Example 4 at $t = t_{N_t}$ for $J_x = J_t = 5$. (6b) Comparison of exact and approximate solution of $u_2(x,t)$ at $t = t_{N_t}$ for $J_x = J_t = 5$

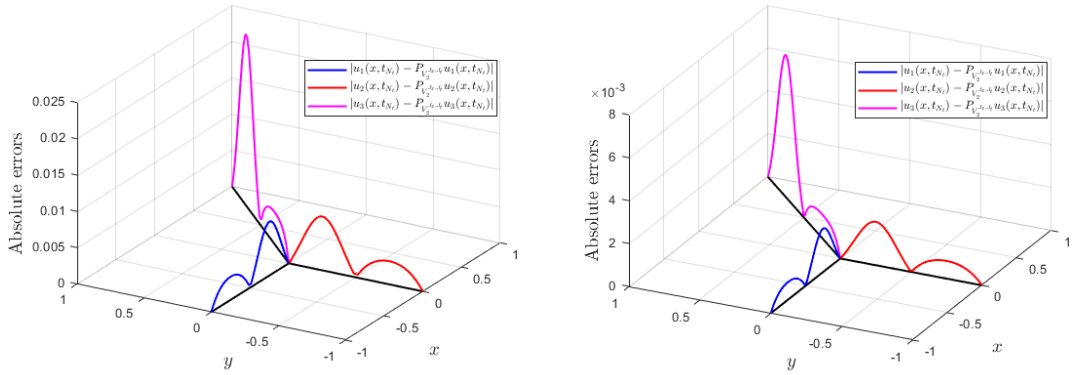

(a) (b)

Fig. 7: Impact of resolution parameters J_x, J_t on AEs obtained for $u(x,t)$ of Example 4 at $t = t_{N_t}$: (7a) for $J_x = J_t = 4$, (7b) for $J_x = J_t = 5$

The analytical solutions of Example 5 are given by

$$u_1(x,t) = u_2(x,t) = t\sin\pi x,$$
$$u_3(x,t) = -2t\sin\pi x.$$

The source functions $f_r(x,t)$, $r = 1,2,3$ can be calculated with the assistance of the exact solutions. The MAE and RMSE are presented in Table 5. As evident from the table, the computational results align well with the theoretical findings. Specifically, increasing the resolution levels $(J_x,;J_t)$ leads to convergence of the approximate solution toward the analytical solution. A linear transformation $w = ax+b$ is applied to approximate the solution over a larger domain. For example, in equations (25) and (27), x is replaced with $\frac{x}{2}$, and the same procedure was used to determine the integration of Haar wavelet and implement the numerical method for the approximate solution. Figures 8a and 8b illustrate the approximate and exact solutions for $J = 5$ in the larger domain $(x,t) \in (0,2)\times(0,2)$. The close similarity between the graphs of the exact and approximate solutions demonstrates the accuracy of the proposed method in larger domains.

Table 5: Effect of J_x, J_t on the obtained MAEs and RMSEs of Example 5.

$J_x = J_t$	$\varepsilon^{1,\infty}_{J_x,J_t} = \varepsilon^{2,\infty}_{J_x,J_t}$	$\varepsilon^{3,\infty}_{J_x,J_t}$	CPU	$\varepsilon^{1,2}_{J_x,J_t} = \varepsilon^{2,2}_{J_x,J_t}$	$\varepsilon^{3,2}_{J_x,J_t}$	CPU
1	$9.2363e-02$	$1.8472e-01$	0.02	$2.4043e-01$	$4.8086e-01$	0.03
2	$4.1649e-02$	$8.3299e-02$	0.03	$1.5574e-01$	$3.1148e-01$	0.03
3	$1.1999e-02$	$2.3998e-02$	0.04	$8.1946e-02$	$1.6389e-01$	0.04
4	$3.1288e-03$	$6.2576e-03$	0.21	$4.1471e-02$	$8.2943e-02$	0.20
5	$7.9348e-04$	$1.5869e-03$	2.98	$2.0797e-02$	$4.1595e-02$	3.06

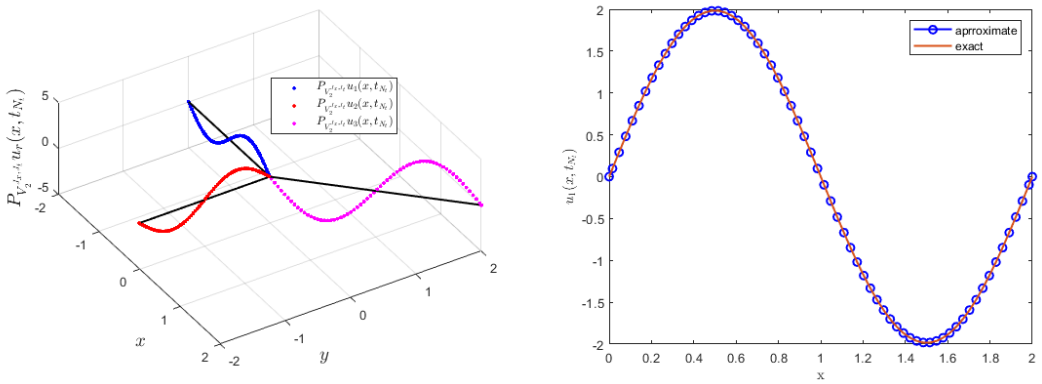

(a) (b)

Fig. 8: (8a) Graph of $P_{V_2^{J_x,J_t}} u_r(x,t)$, $r = 1,2,3$ of Example 5 at $t = t_{N_t}$ for $J_x = J_t = 5$. (8b) Graphical comparison of analytic and approximate solutions of $u_1(x,t)$ at $t = t_{N_t}$ for $J_x = J_t = 5$

8 Conclusion

In this paper, we have examined the neutral delay differential equations on the metric star graph. As the authors know, NDDEs on a metric star graph have never been numerically studied. NDDE-MSG is approximated with Haar wavelet collocation method. This method converts NDDE-MSG into a set of algebraic equations that can easily be solved for the wavelet coefficients. One can obtain the approximate solution by plugging in these coefficients. A convergence analysis determines that the proposed method converges exponentially, thus justifying its theoretical application. We have solved some numerical examples using the proposed method, and the results are presented in Tables 1-5. When the resolution parameters J_x, J_t are increased, the MAEs and RMSEs drop significantly. Figures 2a, 4a, and 6a illustrate numerical solutions, whereas Figures 2b, 4b, 6b and 8b compare accurate and approximate solutions. When comparing the graphs of accurate and approximate wavelet solutions, we can see that the proposed method is effective. As shown in Figures 3, 5, and 7, resolution parameters have an impact on AEs as well. It can be seen from these graphs that the associated AEs are significantly reduced as the convergence parameters J_x, J_t are increased.

Acknowledgement

The authors are thankful to anonymous reviewers for their comments and fruitful suggestions which improved the quality and presentation of the paper.

Financial disclosure

None reported.

Conflict of interest

The authors declare no potential conflict of interests.

Availability of data

Not applicable.

Supporting information

Not applicable.

References

1. Abou-El-Ela, A., Sadek, A., Mahmoud, A.: Existence and uniqueness of a periodic solution for third-order delay differential equation with two deviating arguments. IAENG Int. J. Appl. Math **42**(1), 7–12 (2012)
2. Antoine, J.P., Murenzi, R., Vandergheynst, P., Ali, S.T.: Two-Dimensional Wavelets and their Relatives. Cambridge University Press (2008)
3. Azin, H., Heydari, M., Baghani, O., Mohammadi, F.: Fractional Vieta-Fibonacci wavelets: application for systems of fractional delay differential equations. Physica Scripta **98**(9), 095242 (2023)

4. Dumrongpokaphan, T., Lenbury, Y., Ouncharoen, R., Xu, Y.: An intracellular delay-differential equation model of the HIV infection and immune control. Math. Modell. Natural Phenom. **2**(1), 84–112 (2007)
5. Faheem, M., Khan, A.: A collocation method for time-fractional diffusion equation on a metric star graph with η edges. Math. Meth. Appl. Sci. **46**(8), 8895–8914 (2023)
6. Faheem, M., Khan, A., Oruç, Ö.: A generalized Gegenbauer wavelet collocation method for solving p-type fractional neutral delay differential and delay partial differential equations. Math. Sci. **18**, 137–166 (2024). DOI https://doi.org/10.1007/s40096-022-00490-0
7. Faheem, M., Raza, A., Khan, A.: Collocation methods based on Gegenbauer and Bernoulli wavelets for solving neutral delay differential equations. Math. Comput. Simul. **180**, 72–92 (2020)
8. Ghosh, U., Chowdhury, S., Khan, D.K.: Mathematical modelling of epidemiology in presence of vaccination and delay. Comput. Sci. Infor. Tech. (CS and IT) pp. 91–98 (2013)
9. Gopalsamy, K.: Stability and Oscillations in Delay Differential Equations of Population Dynamics, vol. 74. Springer Science & Business Media Dordrecht (2013)
10. Graef, J.R., Grammatikopoulos, M.K., Spikes, P.W.: On the asymptotic behavior of solutions of a second order nonlinear neutral delay differential equation. Jour. Math. Anal. Appl. **156**(1), 23–39 (1991)
11. Heydari, M.H., Bavi, O.: An efficient wavelet method for nonlinear problems arising in heat transfer. Eng. Comput. **38**(4), 2867–2878 (2022)
12. Heydari, M.H., Razzaghi, M.: A hybrid method based on the Chebyshev cardinal functions/wavelets for time fractional coupled Klein–Gordon–Schrödinger equations. Jour. Comput. Appl. Math. **427**, 115142 (2023)
13. Heydari, M.H., Razzaghi, M.: A new wavelet method for fractional integro-differential equations with ψ-Caputo fractional derivative. Math. Comput. Simul. **217**, 97–108 (2024)
14. Heydari, M.H., Razzaghi, M., Cattani, C.: Fractional Chebyshev cardinal wavelets: application for fractional quadratic integro-differential equations. Inter. Jour. Comput. Math. **100**(3), 479–496 (2023)
15. Hussain, A., Kanwal, T.: Existence and uniqueness for a neutral differential problem with unbounded delay via fixed point results. Trans. A. Razmadze Math. Inst. **172**(3), 481–490 (2018)
16. Insperger, T.: On the approximation of delayed systems by Taylor series expansion. Jour. Comput. Nonlinear Dyn. **10**(2), 024503 (2015)
17. Jackiewicz, Z.: Existence and uniqueness of solutions of neutral delay-differential equations with state dependent delays. Funkcial. Ekvac **30**(1), 9–17 (1987)
18. Kron, G.: Electric circuit models of the Schrödinger equation. Phys. Rev. **67**(1-2), 39 (1945)
19. Lagnese, J.E., Leugering, G.: Domain in Decomposition Methods in Optimal Control of Partial Differential Equations. 148. Springer Science & Business Media (2004)
20. Leugering, G.: Dynamic domain decomposition of optimal control problems for networks of strings and Timoshenko beams. SIAM J. Contr. Optim. **37**(6), 1649–1675 (1999)
21. Mehra, M., Shukla, A., Leugering, G.: An adaptive spectral graph wavelet method for PDEs on networks. Adv. Comput. Math. **47**(1), 1–29 (2021)
22. Mugnolo, D.: Semigroup Methods for Evolution Equations on Networks, vol. 20. Springer (2014)
23. Oruç, Ö.: Integrated Chebyshev wavelets for numerical solution of nonlinear one-dimensional and two-dimensional Rosenau equations. Wave Motion **118**, 103107 (2023)
24. Rahimkhani, P., Ordokhani, Y., Sabermahani, S.: Bernoulli wavelet least squares support vector regression: Robust numerical method for systems of fractional differential equations. Math. Meth. Appl. Sci. **46**(17), 17641–17659 (2023)
25. Raza, A., Khan, A., Sharma, P., Ahmad, K.: Solution of singularly perturbed differential difference equations and convection delayed dominated diffusion equations using Haar wavelet. Math. Sci. **15**(2), 123–136 (2021)
26. Rihan, F.A.: Delay Differential Equations and Applications to Biology. Springer (SP) (2021, https://doi.org/10.1007/978-981-16-0626-7)
27. Ruedenberg, K., Scherr, C.W.: Free-electron network model for conjugated systems. I. Theory. The Jour. Chem. Phy. **21**(9), 1565–1581 (1953)
28. Sabermahani, S., Ordokhani, Y., Rahimkhani, P.: Application of generalized Lucas wavelet method for solving nonlinear fractal-fractional optimal control problems. Chaos, Solitons & Fractals **170**, 113348 (2023)
29. Sabermahani, S., Ordokhani, Y., Razzaghi, M.: Ritz-generalized Pell wavelet method: Application for two classes of fractional pantograph problems. Commun. Nonlinear Sci. Numer. Simul. **119**, 107138 (2023)
30. Shukla, A., Mehra, M., Leugering, G.: A fast adaptive spectral graph wavelet method for the viscous Burgers' equation on a star-shaped connected graph. Math. Meth. Appl. Sci. **43**(13), 7595–7614 (2020)
31. Steinbach, M.C.: On PDE solution in transient optimization of gas networks. Jour. Comput. Appl. Math. **203**(2), 345–361 (2007)
32. Walnut, D.F.: An Introduction to Wavelet Analysis. Springer Science & Business Media (2002)
33. Yoshioka, H., Unami, K., Fujihara, M.: Burgers type equation models on connected graphs and their application to open channel hydraulics (Mathematical Aspects and Applications of Nonlinear Wave Phenomena). Kyuto Uni. **1890**, 160–171 (2014). URL `http://hdl.handle.net/2433/195771`